THE IIOAB JOURNAL

VOLUME 5 : NO 3 : OCTOBER 2014 : ISSN 0976-3104

Institute of Integrative Omics and Applied Biotechnology Journal

Dear Esteemed Readers, Authors, and Colleagues,

I hope this letter finds you in good health and high spirits. It is my distinct pleasure to address you as the Editor-in-Chief of Integrative Omics and Applied Biotechnology (IIOAB) Journal, a multidisciplinary scientific journal that has always placed a profound emphasis on nurturing the involvement of young scientists and championing the significance of an interdisciplinary approach.

At Integrative Omics and Applied Biotechnology (IIOAB) Journal, we firmly believe in the transformative power of science and innovation, and we recognize that it is the vigor and enthusiasm of young minds that often drive the most groundbreaking discoveries. We actively encourage students, early-career researchers, and scientists to submit their work and engage in meaningful discourse within the pages of our journal. We take pride in providing a platform for these emerging researchers to share their novel ideas and findings with the broader scientific community.

In today's rapidly evolving scientific landscape, it is increasingly evident that the challenges we face require a collaborative and interdisciplinary approach. The most complex problems demand a diverse set of perspectives and expertise. Integrative Omics and Applied Biotechnology (IIOAB) Journal has consistently promoted and celebrated this multidisciplinary ethos. We believe that by crossing traditional disciplinary boundaries, we can unlock new avenues for discovery, innovation, and progress. This philosophy has been at the heart of our journal's mission, and we remain dedicated to publishing research that exemplifies the power of interdisciplinary collaboration.

Our journal continues to serve as a hub for knowledge exchange, providing a platform for researchers from various fields to come together and share their insights, experiences, and research outcomes. The collaborative spirit within our community is truly inspiring, and I am immensely proud of the role that IIOAB journal plays in fostering such partnerships.

As we move forward, I encourage each and every one of you to continue supporting our mission. Whether you are a seasoned researcher, a young scientist embarking on your career, or a reader with a thirst for knowledge, your involvement in our journal is invaluable. By working together and embracing interdisciplinary perspectives, we can address the most pressing challenges facing humanity, from climate change and public health to technological advancements and social issues.

I would like to extend my gratitude to our authors, reviewers, editorial board members, and readers for their unwavering support. Your dedication is what makes IIOAB Journal the thriving scientific community it is today. Together, we will continue to explore the frontiers of knowledge and pioneer new approaches to solving the world's most complex problems.

Thank you for being a part of our journey, and for your commitment to advancing science through the pages of IIOAB Journal.

Yours sincerely,

Vasco Azevedo

Vasco Azevedo, Editor-in-Chief
Integrative Omics and Applied Biotechnology
(IIOAB) Journal

Prof. Vasco Azevedo
Federal University of Minas Gerais
Brazil

Editor-in-Chief

Integrative Omics and Applied Biotechnology (IIOAB) Journal Editorial Board:

ISSN: 0976-3104
REGULAR ISSUE
Oves et al.

THE IIOAB JOURNAL

RESEARCH ARTICLE OPEN ACCESS

PRODUCTION OF PLANT-GROWTH PROMOTING SUBSTANCES BY NODULE FORMING SYMBIOTIC BACTERIUM RHIZOBIUM SP. OS1 IS INFLUENCED BY CuO, ZnO AND Fe_2O_3 NANOPARTICLES

Mohammad Oves[1], Mohammad Saghir Khan[1], Almas Zaidi[1], Arham S. Ahmed[2], Ameer Azam[2,3]

[1]Center of Excellence in Environmental Studies (CEES), King Abdulaziz University, Jeddah 21589, Kingdom of SAUDI ARABIA
[2]Department of Agricultural Microbiology, Faculty of Agricultural Sciences, Aligarh Muslim University, U.P. INDIA
[3] Department of Applied Physics, Aligarh Muslim University, UP, INDIA

ABSTRACT

Symbiotic nitrogen fixing rhizobia besides fixing atmospheric nitrogen also produces plant growth promoting substances such as indole acetic acids, siderophores, and cyanogenic compounds etc. However, the effects of nanomaterials on plant growth regulating substances synthesized by these bacteria are not reported. In this paper we have examined the impact of varying concentration of three metal oxide nanoparticles (MONPs) namely copper oxide (CuO), iron oxide (Fe_2O_3) and zinc oxide (ZnO) on growth behaviour and plant growth promoting activities of nodule forming bacterium Rhizobium sp. strain OS1. The three MONPs tested in this study differentially affected the levels of plant growth regulating substances in a dose dependent manner which varied with species of each nanoparticle. A maximum reduction in indole acetic acid, hydrogen cyanide, ammonia and siderophores, expressed by Rhizobium sp. OS1 was observed at 150 μgml^{-1} each of CuO, Fe_2O_3 and ZnO. Iron oxide did not show any toxicity to siderophores. At 50 μgml^{-1}, CuO induced the IAA production by 11% which decreased progressively with increasing concentrations. The synthesis of HCN and NH_3 was completely abolished when strain OS1 was grown with 150 μgml^{-1} of all nanoparticles. Unlike plant growth promoting substances, the production of exo-polysaccharide increased gradually with increasing concentration of each MONPs by rhizobial strain. This study suggests that the nanoparticles of different functional groups affect the physiological expression of rhizobial species differently and it further opens up a new vistas to better understand the impact of nanoparticles on symbiotic interaction between rhizobia and legumes.

Received on: 8th-May-2012
Revised on: 14th-Apr-2014
Accepted on: 21st– Apr-2014
Published on: 18th –Oct-2014

KEY WORDS

Rhizobium, MONPs, Siderophore, IAA, HCN, NH_3

***Corresponding author:** Email: owais.micro@gmail.com Tel: +919045012735, +966590619595

[I] INTRODUCTION

Recently, nanoscience has become one of the most promising fields of research with greater impact on economy and environment health. The research on nanomaterials: materials of 100 nm in at least one dimension, is likely to result in the production of huge number of new nano-products in the coming years. Considering the importance of nanotechnology, a greater attention has been paid on this industry which is expected to reach a market size of approximately 2.6 trillion dollars by 2015 [1]. In addition, nanotechnology is also likely to influence agricultural research especially in (i) the conversion of agricultural and food wastes to energy and other useful by-products through enzymatic nano-bio-processing (ii) disease prevention and treatment of plants using various nanomaterials [2] and (iii) reproductive science and technology. Despite these benefits, the increasing numbers of commercial products, from cosmetics to medicine and fertilizers to crop products are adding sufficient amounts of nanomaterials ultimately to soils. Such nanoparticles have however, been found highly resistant to degradation and persist in soil or water bodies. Nanomaterials for example carbon nanotubes [3, 4], graphene-based nanomaterials [5], iron-based nanoparticles [6], silver [7] and copper, zinc and titanium oxide nanoparticles [8, 9] have been reported to cause biologically undesirable toxic effects on both deleterious (DRMOs) and beneficial rhizosphere microorganisms [10-12] including *Escherichia coli*, *Bacillus subtilis*, and *Streptococcus aureus* [13], *Pseudomonas chlororaphis* [14-18], *Pseudomonas putida* [11] and *Campylobacter jejuni* [19]. However, the reports on the effect of nanoparticles on secondary metabolites of microbes are conflicting. For example, Dimkpa et al. [16] in a recent study found that sub-lethal levels of CuONPs reduced the secretion of plant growth promoting substance siderophore in *P. chlororaphis* O6 whereas ZnO NPs increased the production of the fluorescent siderophore pyoverdine. Similarly, a contrasting effect of CuO and ZnO NPs on siderophores and IAA has also been reported by Dimpka et al. [18] suggesting that the effect of NPs on secondary metabolite production by bacterial populations cannot be generalized rather it is highly

THE IIOAB JOURNAL
ISSN: 0976-3104

metabolite/nano specific and may vary from organisms to organisms. In addition, the nanomaterials are also affecting the human health very negatively [20-22] especially by damaging the macromolecules like DNA [23] and other cellular functions [24].

Therefore, a better understanding of how nanomaterials affect microorganisms is likely to improve the environment health including soil ecosystem. Even-though the symbiotic nitrogen fixers in general are reported to transform atmospheric nitrogen to usable forms of N, the effect of nanoparticles on secondary metabolites of rhizobia is not known. Considering both the positive and negative aspect of the nanomaterials and lack of information on the impact of nanoparticles on the plant growth promoting activities of rhizobacteria, here, we examined the effects of metal oxide nanoparticles like CuO, Fe_2O_3 and ZnO on the growth characteristics and production of plant growth regulating substances by symbiotic nitrogen fixing bacterium *Rhizobium sp*. OS1.

[II] MATERIALS AND METHODS

2.1. Rhizobial strains

A total of 20 rhizobial strains were recovered from the rhizosphere of chickpea (*Cicer arietinum*) plants grown in the experimental fields of Faculty of Agricultural Sciences, Aligarh Muslim University, Aligarh, India. About one gram of soil samples was serially diluted using 50 mM phosphate buffer and spread over yeast extract mannitol agar (YMA) plates amended with Congo-red dye. The plates were incubated at 30±2℃ for three days. The rhizobial strains were characterized biochemically and morphologically. Further, most promising plant growth promoting rhizobial isolate was characterized molecularly by 16S rDNA sequence analysis. The *Rhizobium*-chickpea specificity was further determined by nodulation test [25] using chickpea as a host legume plant.

2.2. Synthesis of metal oxide nanoparticles

In the present investigation, metal oxide nanoparticles were synthesized using metal nitrates. For this, the nitrates of Zn, Cu and Fe and citric acid were dissolved in distilled water with a molar ratio of 1:1. The solutions were stirred with magnetic stirrer at 100^0C. Stirring continued for approximately 2h until the gels were formed. Thereafter, gel was allowed to burn at 200 ^{0}C. A light fluffy mass produced as a result of combustion was annealed further at 400 ^{0}C for one hour to achieve the respective crystalline metal oxide nanoparticles [26].

2.3. Nanoparticles suspension

In this study, 20 nm size metal oxide nanoparticles (MONPs) were used. All metal oxide nanoparticles namely, copper oxide (CuO), iron oxide (Fe_2O_3) and zinc oxide (ZnO) were obtained from the Department of Applied Physics, Excellence centre of Nanoscience, Aligarh Muslim University, Uttar Pradesh, India. For stock solution preparation, 12.5, 25, 50, 100 and 150 mg MONPs were mixed with 100 ml. ultrapure water in 250 ml capacity flask and vigorously stirred for 15 min. After sonicating the sample for 30 min. the resulting suspension was collected and stored at 4 ℃ for further studies.

2.4. Tolerance level of nanoparticles

The rhizobial strains were tested for their sensitivity/tolerance to chemically and functionally diverse MONPs CuO, Fe_2O_3 and ZnO, by agar plate dilution method. The freshly prepared agar plates were amended separately with increasing concentrations (0 to 300 μgml^{-1}) of nanoparticles. Plates were incubated at 30±2℃ overnight to check the sterility of the medium. Later, plates were spot inoculated with loopful rhizobial culture (10 µl of 108 cells ml^{-1}). Plates were incubated at 30^0 (SE=2℃) for three days and the highest concentration of each nanoparticle supporting rhizobial growth was defined as the maximum tolerance level (MTL).

2.5. Growth pattern

For the determination of growth pattern, a 0.5 ml of the culture (10^8 cells ml^{-1}) of freshly grown *Rhizobium sp*. OS1 was inoculated into 100 ml yeast extract mannitol broth medium containing 0 (control) to 150 μgml^{-1} nanoparticles of CuO, Fe_2O_3 and ZnO, separately. The cultures were incubated at 30±2℃ on a rotary shaker with 120 r/min. At regular intervals, the optical density was measured at 600 nm using a spectrophotometer (Spectronic 20, USA). The rhizobial growth curve was obtained by plotting the optical density as a function of time.

2.6. Indole acetic acid assay

Indole-3-acetic acid (IAA) synthesized by *Rhizobium sp*. OS1 strain was quantitatively estimated by the method of Gordon and Weber [26], later modified by Brick et al. [27]. For this activity, the rhizobial strains were grown in Luria Bertani broth (gl^{-1}: tryptone 10; yeast extract 5; NaCl 10 and pH 7.5). Luria Bertani broth (100 ml) having a fixed concentration of tryptophan (100 μgml^{-1}) was treated with 0, 12.5, 25, 50, 100 and 150 μgml^{-1} of CuO, Fe_2O_3 and ZnO, separately. A 0.1 ml (10^8cells ml^{-1}) of rhizobial strains was inoculated into each separate flask and was incubated for three days at 30℃ (SE=2℃) with shaking at 120 r/min. After three days, five mil culture from each treatment was removed and centrifuged (5433) for 15 min. and an aliquot of 2 ml supernatant was mixed with 100 µl of orthophosphoric acid and 4 ml of Salkowsky reagent (2% 0.5 M $FeCl_3$ in 35% perchloric acid) and incubated at 30^0C (SE=2℃) in darkness for 1 h. The absorbance of pink colour was read at 530 nm. The IAA concentration in the supernatant was determined using a calibration curve of pure IAA as a standard.

2.7. Siderophores assay

The *Rhizobium sp*. OS1 strain was further tested for siderophores production using Chrome Azurol S (CAS) agar medium following the method of Alexander and Zuberer [28]. Chrome Azurol S agar plates supplemented with 0, 12.5, 25, 50,100 and 150 μgml^{-1} of each nanoparticles were prepared separately and spot inoculated with loop full fresh culture (10 µl of 108 cells ml^{-1}) and incubated at 30℃ (SE=2℃) for three days. Development of yellow to orange halo around the bacterial growth was considered as positive indicator of siderophores-biosynthesis. The production of siderophores by the test strains was further detected quantitatively using Modi medium (K_2HPO_4 0.05%; $MgSO_4$ 0.04%; NaCl 0.01%; mannitol 1%; glutamine 0.1% and NH_4NO_3 0.1%) [29]. Modi medium amended with 0, 12.5, 25, 50, 100 and 150 μgml^{-1} of each metal oxide nanoparticles was inoculated with 108 bacterial cells ml^{-1} and incubated at 30 ℃(SE=2℃) for three days. Catechol type phenolates were measured on ethyl acetate extracts of the culture supernatant using a modification of the ferric chloride-ferricyanide reagent of Hathway [29]. Ethyl acetate extracts were prepared by extracting 20 ml of supernatant three times with an equal volume of the solvent at pH_2. Hathway's reagent was prepared by adding one milliliter of 0.1 M ferric chloride in 0.1 NHCl to 100 ml of distilled water, and to this, was added 1 ml of 0.1M potassium ferricyanide [30]. For the assay, one volume of the reagent was added to one volume of the sample and the absorbance was determined at 560 nm for salicylic acid (SA) with sodium salicylate as a standard and at 700 nm for

THE IIOAB JOURNAL
ISSN: 0976-3104

dihydroxy phenols with 2,3-dihydroxy benzoic acid (DHBA) as a standard.

2.8. Assay of hydrogen cyanide and ammonia

Hydrogen cyanide (HCN) production by *Rhizobium sp*. OS1 strain was detected by the method of Bakker and Schipper [30]. For HCN production, rhizobial strains were grown on an HCN induction medium (gl^{-1}: tryptic soy broth 30; glycine 4.4 and agar 15) supplemented with 0, 12.5, 25, 50, 100 and 150 μgml^{-1} of each metal oxide nanoparticles at 30℃(SE=2℃) for five days. Further, 100 µl of 108 cells ml^{-1} of freshly grown culture of *Rhizobium sp*. OS1 strain was spread on Petri plates. A disk of Whatman filter paper No. 1 dipped in 0.5% picric acid and 2% Na_2CO_3 was placed at the lid of the Petri plates. Plates were sealed with parafilm. After four days incubation at 30℃ (SE=2℃), red/orange brown colour of the paper indicating HCN production was observed. For ammonia (NH_3) assessment, the *Rhizobium sp*. OS1 strain was grown in peptone water with 0, 12.5, 25, 50, 100 and 150 µg/ml of each metal oxide nanoparticles and incubated at 30℃(SE=2℃) for five days. One milliliter of Nessler reagent [potassium iodide 50 g; distilled water (ammonia free) 35 ml; mixed with saturated aqueous solution of mercuric chloride until a slight precipitate developed; potassium hydroxide 400 ml; diluted the solution to 1000 ml with ammonia free distilled water; allowed it to stand for one week, decanted supernatant liquid and stored in a tightly capped amber bottle] was added to each tube and the development of yellow colour indicating ammonia production was recorded following the method of Dye [31].

2.9. Exo-polysaccharides production

Exo-polysaccharide (EPS) produced by the *Rhizobium sp*. OS1 was determined as suggested by Mody et al. [32]. For this, the bacterial strains were grown in 100 ml capacity flasks containing yeast extract mannitol broth medium supplemented with 10% sucrose and treated with 0, 12.5, 25, 50, 100 and 150 μgml^{-1} of each metal oxide nanoparticles. Inoculated flasks were incubated for five days at 30 ℃(SE=2℃) on rotary shaker at 120 r/min. Culture broth was spun (5433 g) for 30 min., and EPS was extracted by adding three volumes of chilled acetone (CH_3COCH_3) to one volume of supernatant. The precipitated EPS was repeatedly washed three times alternately with distilled water and acetone, transferred to a filter paper and weighed after overnight drying at room temperature. Each individual experiment was repeated three times.

2.10. Statistical analysis

The experiments were repeated three times using the same treatments. The difference among treatment means was compared by high range statistical domain (HSD) using Tukey test ($p \leq 0.05$).

[III] RESULTS AND DISCUSSION

3.1. Nanoparticles-tolerance and identification of bacterial strain

Symbiotically nitrogen fixing bacterial strain *Rhizobium sp*. OS1 demonstrated a variable MONPs tolerance and when tested exhibited different PGP activities under in vitro environment. The MTL values of CuO, Fe_2O_3 and ZnO was 160, 190, and 155 μgml^{-1}, respectively. The variation in tolerance to certain MONPs tested in this study could probably be due to differences in the interaction of physiological products of rhizobial strain with varying species of MONPs. Also, the genetic makeup of this strain might have played an important role in tolerating the MONPs. The toxicity of nanoparticles has however, been reported to be affected by many factors including types and chemical composition of metals, size of particles [33], shape of particles [34], surface charge [6] and bacterial strains [19]. In similar studies, bacteria *Cupriavidus metallidurans* and *E. coli* have been found highly sensitive to higher concentrations of metal oxide nanoparticles such as TiO_2 or Al_2O_3 NP [35]. In a follow up study, Khan et al. [36] isolated nanoparticles tolerant bacterium *Aeromonas punctata* from sewage environment which was able to tolerate 200 µg/ml AgNPs while Li et al. [37] in a similar study identified a Gram negative bacterium *Pseudomonas putida* which could tolerate >500 µgml-1 zinc oxide nanoparticle. Of the total 20 rhizobial strains recovered from the chickpea rhizosphere and identified using morphological and biochemical tests and nodulation test, nanoparticle tolerant strain OS1 was further characterized by amplification of ribosomal 16S rDNA sequence. The resulting base sequence was compared with those of some related organisms by BLASTn analysis. An 1189 bp sequence demonstrated 99% similarity with *Rhizobium* species. The sequence was deposited in the EMBL database under accession numbers HE663761 so that it remains in the public domain.

3.2. Growth pattern of rhizobial strain in the presence of MONPs

The growth pattern of *Rhizobium* species was observed while growing strain OS1 in the presence of 0 (control) to 150 µgml-1 nanoparticles of CuO, Fe_2O_3 and ZnO, added separately to nutrient broth medium. The variation in rhizobial growth was monitored after every two hours intervals. The bacterial growth decreased with increasing concentration of each individual MONPs **[Supplementary figure–1]**. Among the tested MONPs, CuO at 150 μgml^{-1} was highly toxic and decreased the bacterial growth by 68 % compared to rhizobial strain OS1 grown in MNOPs free medium. While comparing the effect of only 150 µgml-1 of different MNOPs on rhizobial growth, the order of toxicity was: CuO>ZnO>Fe_2O_3. Although, the exact mechanism as to how the MNOPs kills the bacterial cell is not conclusively known but the inhibition may be caused by the interaction of MNOPs with the bacterial membrane causing pitting of the cell wall, dissipation of the proton motive force, and consequently the cell death [38]. In addition, nanoparticles have also been reported to interact with bacterial DNA leading to the DNAs replication damage [39, 40]. These observations agree with those of the previous work reported by Beak and An [13] where CuO NPs was found most inhibitory against *E. coli*, *B. subtilis*, and *S. aureus* than ZnO. In a similar report, Jones et al. [10] also determined the detrimental effect of ZnO against broad spectrum microorganisms.

THE IIOAB JOURNAL
ISSN: 0976-3104

3.3. Plant growth promoting activities of rhizobial strain

3.3.1. Siderophore production under MONPs-stress

Siderophore, a low molecular weight iron chelating peptide released by majority of Gram negative bacterial strains is one of the most important biological traits that provide protection to plants by making the accessibility of iron difficult to phytopathogens. On the other hand, iron is essentially required by bacteria for its effective metabolic activity. However, there is acute scarcity of iron due to its ability of insolubility at neutral to alkaline pH [41]. In order to challenge this elemental problems, majority of bacteria belonging to both Gram positive and Gram negative groups have evolved mechanism wherein they secrete siderophores to scavenge iron in iron deficient environment [42-45]. This exceptional quality of bacteria to secrete chemically diverse class of siderophores is likely to help bacterial communities to survive better in an iron-deficient environment. Therefore, considering the importance of siderophore, we determined the synthesis of secondary metabolites: siderophores, by the MONPs tolerant *Rhizobium sp*. OS1 using CAS agar plates treated differently with varying concentration of the nanomaterials **[Supplementary table– 2]**. *Rhizobium sp*. OS1 produced a 13 mm orange zone, an indicator of siderophore production, on MNOPs free CAS agar plate. The size of the zone was however decreased significantly ($p \leq 0.05$) when MONPs were added to CAS agar plates. Generally, the effects of MONPs were less at lower concentrations of each MONPs which became more pronounced at the higher rates of MONPs. Accordingly, when the effect of varying concentrations of MNOPs on siderophore production were compared, a maximum of 61% decrease in zone size was recorded at 150 μgml^{-1} each of CuO and ZnO over control while any tested concentration of Fe_2O_3 did not show inhibitory effect on siderophore production **[Supplementary table– 2]**. After qualitative analysis, the production of siderophores was quantitatively assayed. In this regard, the SA and DHBA type siderophores were detected in the culture supernatant of the *Rhizobium sp*. OS1, grown in the Modi medium devoid of nanomaterials **[Supplementary figure– 2a, 2b]**. A nanomaterial concentration dependent progressive decline for both iron binding molecules was observed. Indeed, the reduction in siderophores quantity was greatly influenced by the species of MONPs. Of the three MONPs, ZnO at 150 μgml^{-1} was most toxic for the generation of both SA (17.3 μgml^{-1}) and DHBA (9.5 μgml^{-1}) and decreased SA and DHBA synthesis significantly ($p \leq 0.05$) by 49% and 56%, respectively, over control. Furthermore, while comparing the effect of 150 μgml^{-1} each of ZnO and CuO, the ZnO reduced the production of SA and DHBA by 12 and 17% respectively over CuO. Like the qualitative assay, there was no effect of Fe_2O_3 nanomaterial even at 150 µg/ml on SA and DHBA secretion by the strain OS1. In agreement to our findings, Dimkpa et al. [14] observed that the sub-lethal level of CuO NPs decreased the production of the fluorescent siderophore pyoverdine (PVD) by *P. chlororaphis* which could probably be due to the impairment of the genes involved in PVD secretion.

3.4. Impact of MONPs on indole-acetic acid production

The IAA synthesized by the *Rhizobium sp*. OS1 under different concentrations of MONPs was variable **[Supplementary table– 2]**. Generally, the IAA was produced both under normal and MONPs treated and Rhizobium inoculated LB medium but the level of IAA under MONPs was considerably lower compared to those detected in conventional (untreated) medium. For example, *Rhizobium sp*. OS1 produced a significant ($p \leq 0.05$) amount of IAA (43 μgml^{-1}) when grown in medium devoid of MNOPs. Interestingly, the IAA production decreased with increasing concentration of each MNOPs except CuO NPs which induced the synthesis of IAA by 11% up to 50 μgml^{-1}; IAA decreased substantially thereafter. While comparing the impact of higher tested concentration (150 μgml^{-1}) of the three MNOPs, ZnO nanomaterials had greatest deleterious effect on IAA and reduced it by 79% which was 44 and 25% for CuO and Fe2O3, respectively relative to the control. Among different concentrations used in this study, ZnO at 150 μgml^{-1} maximally declined the IAA by 67 % compared to those observed for CuO (33%) and Fe_2O_3 (34%), assayed at 50 μgml^{-1}. While calculating the average value of MONP toxicity on IAA synthesis by strain OS1, ZnO was most toxic (mean value 24.9 μgml^{-1}) and reduce the IAA production by 42% compared to control (43 μgml^{-1}). Based on this, the order of MONP toxicity increased in the order: $ZnO > Fe_2O_3 > CuO$. In a recent study, Dimkpa et al. [15] observed that the amendment of the medium with CuO and ZnO NPs modified IAA levels from those of the control plant growth promoting Gram negative bacterium *P. chlororaphis*. They found that CuO NPs increased the IAA production significantly ($P \leq 0.05$) by 34% in a 48h grown culture while ZnO NPs reduced IAA levels by 79% relative to the control. The extent of inhibition of IAA formation caused by the ZnO NPs was however reduced by co-addition of CuO NPs; the amount of IAA released by bacterial cell grown with mixture of NPs was closer to that of cells grown solely with CuO NPs. Interestingly, the *P. chlororaphis* cells exposed to sub-lethal concentration of CuO NPs was found to metabolize tryptophan more aggressively than cells grown with ZnO NPs. The differential effects of NPs on bacterial metabolisms thus suggest that the nanoparticles may have a specific target in bacterial population.

3.3. Estimation of EPS, HCN and NH_3 under MONPs stress

Among the PGP substances which indirectly facilitates the growth of plants and released by bacterial populations including *Rhizobium* was investigated further in this study by exposing *Rhizobium sp*. OS1 to MONPs. The release of one such compound for example EPS increased significantly ($p \leq 0.05$) when strain OS1 was exposed to progressively increasing

THE IIOAB JOURNAL
ISSN: 0976-3104

concentration of each MONPs added separately to nutrient broth amended with a fixed rate of dextrose ($10gl^{-1}$). Among all the tested MONPs, a more pronounced stimulatory effect on EPS secretion was detected at 150 μgml^{-1} CuO which increased the EPS by 90% compared to control **[Supplementary table– 2]**. While calculating the mean effect of all concentration of each MONPs, CuO NPs was found as a strong inducer of EPS synthesis and enhanced the EPS production by 58% which was followed by Fe_2O_3 (46%) and ZuO (29%). The EPS secreted by bacterial strains has been considered one of the important metabolic traits that protect bacterial cells from the nuisance of adverse environment [46]. It was therefore, very much likely that the rhizobial cells tested in this investigation might have been masked by the toxicity of MONPs by secreting EPS. Moreover, the EPS is reported to protect bacteria against desiccation, dehydration, phagocytosis and phage attack besides supporting N_2 fixation by preventing high oxygen tension. In our previous work we have also observed a similar enhanced production of EPS by rhizobial strains when grown with metal ion [44] and fungicides [47]. Comparable observation on the effects of nanoparticles on EPS secretion by bacterial strain is also reported Wu et al. [48].

The other mechanism by which rhizobacteria protects the growing plants from pathogen attack involves the direct killing of parasites by producing cyanogenic compound HCN [49]. Consequently, the synthesis of such compounds was examined here. Interestingly, the concentrations of CuO, Fe_2O_3 and ZnO up to 100 µg/ml did not affect negatively the HCN and ammonia synthesis by the *Rhizobium sp*. OS1 **[Supplementary table– 2]** while concentration greater than 100 μgml^{-1} of each MONPs had a strong inhibitory effect. In agreement to our report, [45-47] observed the release of cyanogenic compounds like HCN by the rhizobacterial strains into the rhizosphere. The ammonia released by the rhizobacterial strain plays a signaling role in the interaction between rhizobacteria and plants and also increase the glutamine synthetase activity [50]. Therefore, it seems probable that MONPs employed in this study might have inhibited the functioning of the enzymes participating in different metabolic pathways of PGP traits such as SA, DHBA and IAA of the *Rhizobium sp*. OS1 leading to a differential losses in the production of PGP substances.

[IV] CONCLUTION

In conclusion, we have established that the application of nanoparticles differentially modified the production of plant growth promoting substances under in vitro conditions in the nodule forming Gram-negative bacterium *Rhizobium sp*. OS1. Generally, the release of plant promoting substances by rhizobial strain was dose dependent and nanomaterial specific. Therefore, the discharge of nanoparticles in the environment should be carefully monitored so that the loss of both structure and functions of agronomically important microbes could be protected from the toxicity of MONPs. This study also provides a base line data to further understand the symbiotic interaction between legumes and rhizobia in a nanoparticles contaminated environment.

ACKNOWLEDGEMENT

One of the authors Mohammad Oves is grateful acknowledged to Council of Scientific and Industrial Research (CSIR) New Delhi, India for financial assistance in form of senior research fellow.

CONFLICT OF INTEREST

No conflict of interest in the form of either financial or commercial is involved in any way with the present study.

FINANCIAL DISCLOSURE

No financial sponsor in the form of person, institution or organization is involved in the present work.

REFERENCES

[1] Holman M. [2007] Nanomaterials forecast: Volumes and applications. Presented at the ICON Nanomaterial Environmental Health and Safety Research Needs Assessment, Bethesda, MD, USA.

[2] Dreher KL. [2004] Health and environmental impact of nanotechnology: Toxicological assessment of manufactured nanoparticles. *Toxicol Sci* 77:3–5.

[3] Kang S, Pinault M, Pfefferle LD, Elimelech M.[2007] Single-walled carbon nanotubes exhibit strong antimicrobial activity. *Langmuir* 23:8670–8673.

[4] Liu SB, Wei L, Hao L, Fang N, Chang MW, Xu R, Yang YH, Chen Y. [2009] Sharper and faster "nano darts" kill more bacteria: a study of antibacterial activity of individually dispersed pristine single walled carbon nanotube. *ACS Nano* 3:3891–3902.

[5] Hu WB, Peng C, Luo WJ, et al. [2010]Graphene-based antibacterial paper. *ACS Nano* 4:4317–4323.

[6] Auffan M, Achouak W, Rose J, et al. [2008]Relation between the redox state of iron-based nanoparticles and their cytotoxicity towards Escherichia coli. *Environ Sci Technol* 42: 6730–6737.

[7] Sondi I, Salopek-Sondi B. [2004] Silver nanoparticles as antimicrobial agent: a case study on E-coli as a model for Gram-negative bacteria. *J Colloid Inter Sci* 275:177–182.

[8] Kasemets K, Ivask A, Dubourguier, HC, Kahru A. [2009] Toxicity of nanoparticles of ZnO, CuO and TiO2 to yeast Saccharomyces cerevisiae. *Toxicol In Vitro* 23:1116–1122.

[9] Ge Y, Schimel JP, Holden PA. [2011] Evidence for negative effects of TiO2 and ZnO nanoparticles on soil bacterial communities. *Environ Sci Technol* 45:1659–1664.

[10] Jones N, Ray B, Ranjit KT, Manna AC. [2008] Antibacterial activity of ZnO nanoparticle suspensions on a broad spectrum of microorganisms. *FEMS Microbiol Lett* 279:71–61.

[11] [Gajjar P, Pettee B, Britt DW, Huang W, Johnson WP, Anderson AJ. [2009] Antimicrobial activities of commercial nanoparticles against an environmental soil microbe, *Pseudomonas putida* KT2440. *J Biol Eng* 3:9.

[12] Gunawan C, Teoh WC, Marquis CP, Amal R. [2011] Cytotoxic origin of copper(ii) oxide nanoparticles: comparative studies

with micron-sized particles, leachate, and metal salts. *ACS Nano* 5:7214−7225.

[13] Baek YW, An YJ. [2011] Microbial toxicity of metal oxide nanoparticles (CuO, NiO, ZnO, and Sb2O3) to Escherichia coli, Bacillus subtilis, and Streptococcus aureus. *Sci Total Environ* 409:1603−1608.

[14] Dimkpa CO, Zeng J, McLean JE, Britt DW, Zhan J, Anderson AJ. [2012] Production of Indole-3-Acetic Acid via the Indole-3-Acetamide Pathway in the Plant-Beneficial Bacterium Pseudomonas chlororaphis O6 Is Inhibited by ZnO Nanoparticles but Enhanced by CuO Nanoparticles. *Appl Environ Microbiol* 78:1404–1410.

[15] Dimkpa CO, Calder A, McLean, JE, Britt DW, Anderson AJ. [2011]Responses of a soil bacterium, Pseudomonas chlororaphis O6 to commercial metal oxide nanoparticles compared with responses to metal ions. *Environ Pollut* 159:1749−1756.

[16] Dimkpa CO, McLean JE, Britt DW, Anderson AJ. [2012] CuO and ZnO nanoparticles differently affect the secretion of fluorescent siderophores in the beneficial root colonizer Pseudomonas chlororaphis O6. Nanotoxicol., in press DOI: 10.3109/17435390.2011.598246.

[17] Dimkpa CO, McLean JE, Britt DW, et al. [2012] Nanospecific Inhibition of Pyoverdine Siderophore Production in Pseudomonas chlororaphis O6 by CuO Nanoparticles. *Chem. Res.,* in press DOI: 10.1021/tx3000285.

[18] Dimkpa CO, Zeng J, McLean JE, Britt DW, Zhan J, Anderson AJ. [2012] Production of indole-3-acetic acid via the indole-3-acetamide pathway in the plant-beneficial bacterium, Pseudomonas chlororaphis O6 is inhibited by ZnO nanoparticles but enhanced by CuO nanoparticles. *Appl Environ Microbiol* 78:1404−1410.

[19] Xie Y, He Y, Irwin PL, Jin T, Shi X. [2011] Antibacterial activity and mechanism of action of zinc oxide nanoparticles against Campylobacter jejuni. *Appl Environ Microbiol* 77: 2325–2331.

[20] Brumfiel G. [2003] Nanotechnology: a little knowledge. *Nature* 424:246–248.

[21] Service RF. [2003] Nanomaterials show signs of toxicity. *Science* 300: 243.

[22] Service RF. [2004] Nanotechnology grows up. *Science* 304:1732– 1734.

[23] Hirakawa K, Mori M, Yoshida M, Oikawa S, Kawanishi S. (2004) Photo-irradiated titanium dioxide catalyzes site specific DNA damage via generation of hydrogen peroxide. *Free Radi Res 38*:439–447.

[24] Rahman Q, Lohani M, Dopp E. [2000] Evidence that ultrafine titanium dioxide induces micronuclei and apoptosis in Syrian hamster embryo fibroblasts. Environ. *Health Persp* 110:797–800.

[25] Somasegaran P, Hoben HJ, Gurgun V. [1988] Effects of inoculation rate, rhizobial strain competition, and nitrogen fixation in chickpea. *Agron J* 80:68−73.

[26] Gordon S, Weber RP. (2004) The colorimetric estimation of IAA. *Plant Physiol* 26:192–195.

[27] Brick JM, Bostock RM, Silversone SE. [1991] Rapid in situ assay for indole acetic acid production by bacteria immobilized on nitrocellulose membrane. *Appl Environ Microbiol* 57:535–538.

[28] Alexander DB, Zuberer DA. [1991] Use of chrome azurol S reagents to evaluate siderophore production by rhizosphere bacteria. *Biol Fert Soils* 12:39–45.

[29] Reeves MW, Pine L, Neilands JB, Balows A. [1983] Absence of siderophore activity in Legionella species grown in iron-deficient media. *J Bacteriol* 154:324–329.

[30] Bakker AW, Schipper B. [1987] Microbial cyanide production in the rhizosphere in relation to potato yield reduction and Pseudomonas sp. mediated plant growth stimulation. *Soil Biol Biochem* 19:451–457.

[31] Dye DW. [1962] The inadequacy of the usual determinative tests for the identification of Xanthomonas sp. *Nat Sci* 5:393–416.

[32] Mody BR, Bindra MO, Modi VV. [1989] Extracellular polysaccharides of cowpea rhizobia: compositional and functional studies. *Arch Microbiol* 1:2–5

[33] Heinlaan M, Ivask A, Blinova I, Dubourguier HC, Kahru A. [2008] Toxicity of nanosized and bulk ZnO, CuO, and TiO2 to bacteria Vibrio fischeri and crustaceans Daphnia magna and Thamnocephalus platyurus. *Chemosphere* 71:1308–1316.

[34] Pal S, Tak YK, Song JM. [2007] Does the antibacterial activity of silver nanoparticles depend upon the shape of the nanoparticle? A study of the Gram negative Escherichia coli. *Appl Environ Microbiol* 73:1712–1720.

[35] Deckers AS, Loo S, L'hermite MM, et al. [2009] Size-, Composition- and Shape-Dependent Toxicological Impact of Metal Oxide Nanoparticles and Carbon Nanotubes toward Bacteria. *Environ Sci Technol* 43: 8423–8429.

[36] Khan S, Kumar BE, Mukherjee A, Chandrasekaran N. [2011] Bacterial tolerance to silver nanoparticles (SNPs): Aeromonas punctata isola.ted from sewage environment. *J Basic Microbiol* 51:183–90.

[37] Li M, Pokhrel S, Jin X, Mädler L, Damoiseaux R, Hoek EM. [2011] Stability, bioavailability, and bacterial toxicity of ZnO and iron-doped ZnO nanoparticles in aquatic media. *Environ Sci Technol* 15:755–761.

[38] Choi O, Deng KK, Kim NJ, et al. [2008] The inhibitory effects of silver nanoparticles, silver ions, and silver chloride colloids on microbial growth. *Water Res* 42:3066–3074

[39] Rai M, Yadav A, Gade A. [2009] Silver nanoparticles as a new generation of antimicrobials. *Biotechnol Adv* 27:76–83.

[40] Yang W, Shen C, Ji Q, An H, Wang J, Liu Q, Zhang Z .[2009]Food storage material silver nanoparticles interfere with DNA replication fidelity and bind with DNA. *Nanotechnol* 20:085102.

[41] Neilands JB. [1995] Siderophores: structure and function of microbial iron transport compounds. *J Biol Chem* 270:26723−26726.

[42] Poole K, Mckay GA. (2003] Iron acquisition and its control in Pseudomonas aeruginosa: many roads lead to Rome. *Front Biosci* 8:661−686.

[43] Dimkpa C, Merten D, Svatoš A, Büchel G, Kothe E. [2008] Hydroxamate siderophores produced by Streptomyces acidiscabies E13 bind nickel and promote growth in cowpea (Vigna unguiculata L.) under nickel stress. *Can J Microbiol* 54:163−172.

[44] Wani PA, Khan MS.[2011] Heavy metal toxicity and their remediation by soil microbes: effect of heavy metals and their detoxification by plant growth promoting rhizobacteria. LAP Lambert Academic publishing.

[45] Ahemad M, Khan MS. [2012] Effects of pesticides on plant growth promoting traits of Mesorhizobium strain MRC4. *J Sau Soci Agric Sci* 11:63–71.

[46] Ahemad M, Khan MS.[2011] Plant-Growth-Promoting fungicide-tolerant rhizobium improves growth and symbiotic

characteristics of lentil (Lens esculentus) in fungicide-applied soil. *J Plant Growth Regul* 30:334–342.

[47] Ahemad M, Khan MS. [2011] Effect of tebuconazole-tolerant and plant growth promoting Rhizobium isolate MRP1 on pea–Rhizobium symbiosis. *Sci Horticul* 129: 266–272.

[48] Wu B, Husang R, Sahu M, Feng X, Biswas P, Tang YJ. [2010]Bacterial responses to Cu-doped TiO2 nanoparticles. *Sci Total Environ* 408:1755–1758.

[49] Kang BG, Kim WT, Yun HS, Chang SC. [2010] Use of plant growth-promoting rhizobacteria to control stress responses of plant roots. *Plant Biotechnol Rep* 4:179–183.

[50] Chitra RS, Sumitra VC, Yash DS. [2002] Effect of different nitrogen sources and plant growth regulators on glutamine synthetase and glutamate synthase activities of radish cotyledons. *Bulg J Plant Physiol* 28:46–56

.

THE IIOAB JOURNAL
ISSN: 0976-3104

Supplementary Materials (As supplied by authors)

Supplementary Table: 1. General features of the *Rhizobium sp.* OS1

Characteristics	*Rhizobium* sp. OS1
Accession number	HE663761
Morphology	
Shape	Short rod
Gram reaction	_
Biochemical reaction	
Citrate utilization	_
Indole	+
Methyl red	+
Nitrate reduction	+
Voges Proskaur	+
Oxidase	_
Catalase	+
Carbohydrate utilization	
Glucose	+
Lactose	_
Mannitol	+
Sucrose	+
Enzymatic Hydrolysis	
Starch	+
Gelatin	_
Maximum tolerance level to MONPs	
CuO	160 µgml-1
Fe_2O_3	190 µgml-1
ZnO	155 µgml-1

“

+” and “-” sign indicates positive and negative reaction results, respectively

Supplementary Table: 2. Plant growth promoting activities of the *Rhizobium* sp. OS1 influenced by MONPs

MONPs	Concentration (µgml-1)	IAA (µgml-1)	EPS (µgml-1)	Siderophore [zone on CAS agar (mm)]	NH3	HCN
Control	0	43.0±1.0g	18.3±1.0a	13.0±1.0e	+	+
CuO	12.5	46.0±1.0h	21.6±1.5b	12.0±1.0d	+	+
	25	46.6±1.5h	25.3±1.0c	11.0±1.5d	+	+
	50	48.0±1.0h	29.6±1.5d	9.7±1.5c	+	+
	100	40.0±2.0g	33.3±1.5e	8.0±1.5b	+	+
	150	32.1±2.0e	35.0±1.5f	5.0±1.0a	-	-
	Mean	42.5	28.9	9.1		
Fe_2O_3	12.5	42.3±1.5g	20.1±2.5a	13.0±1.0e	+	+
	25	41.0±1.0g	23.0±1.5b	13.0±1.0e	+	+
	50	36.3±1.5f	28.3±1.0c	12.0±1.0d	+	+
	100	29.3±2.3c	30.3±2.1d	11.0±1.0d	+	+
	Mean	34.6	26.7	12.0		
ZnO	12.5	37.3±2.0f	18.6±1.5a	11.0±1.0d	+	+
	25	31.0±1.0e	20.2±1.5a	10.0±1.5c	+	+
	50	27.6±1.5d	24.5±1.0c	9.0±1.0c	+	+
	100	20.0±1.0b	25.0±2.0c	7.0±1.0b	+	+
	150	9.1±1.0a	29.1±1.5d	5.0±1.0a	-	-
	Mean	24.9	23.4	8.4		
	***F* value**	156.73	48.56	16.11		
	LSD	2.484	2.237	1.922		

± indicate standard deviation, + indicates positive and - indicates negative

THE IIOAB JOURNAL
ISSN: 0976-3104

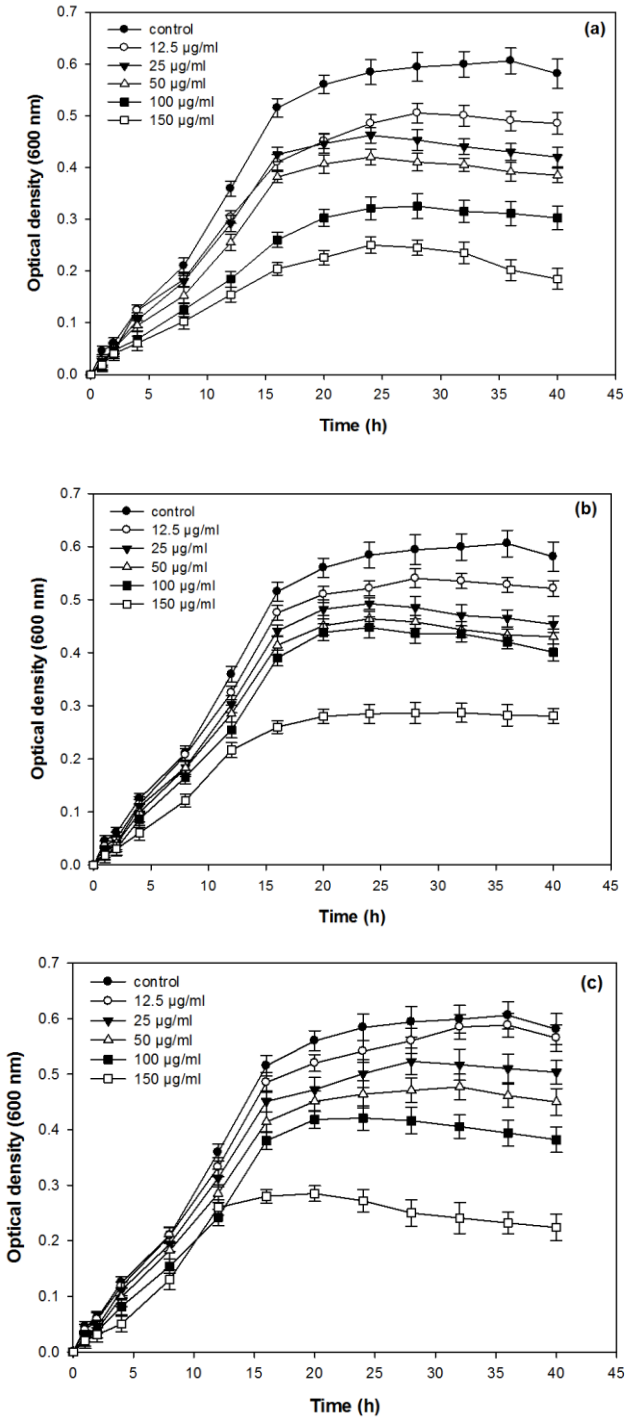

Fig. 1: Impact of varying concentrations of metal oxide nanoparticles (a) CuO (b) Fe2O3 and (c) ZnO on the *Rhizobium sp.* OS1 grown in nutrient broth medium at different time intervals.

THE IIOAB JOURNAL
ISSN: 0976-3104

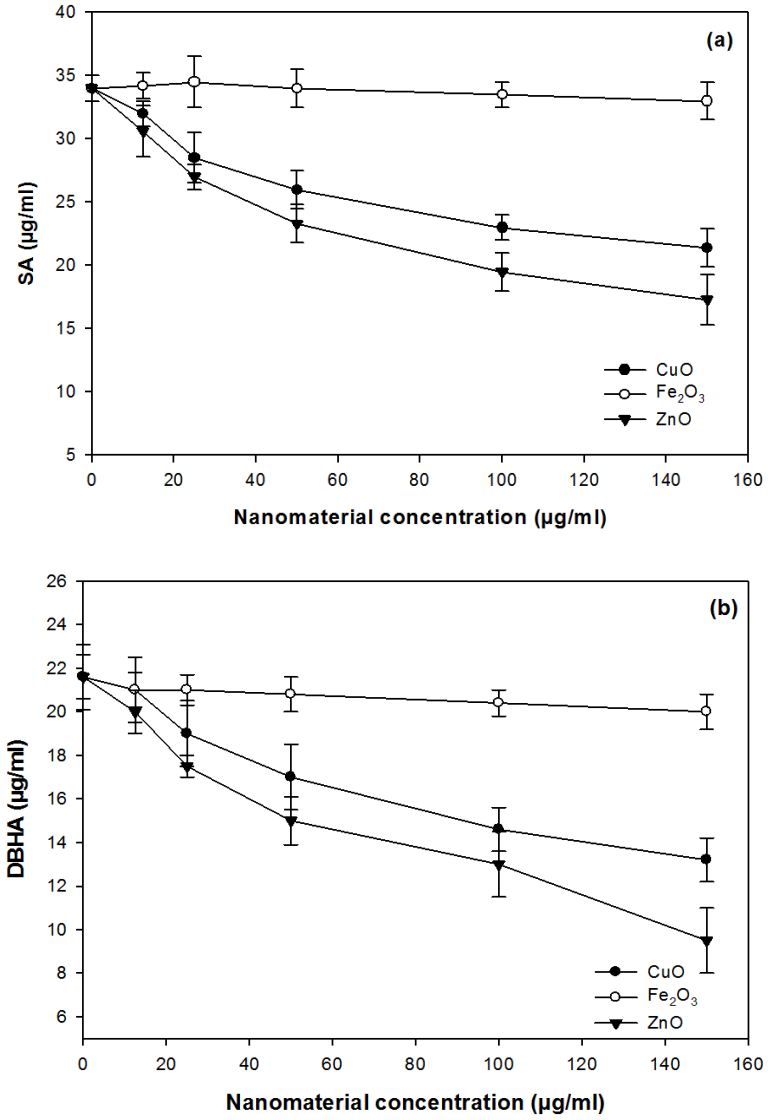

Fig. 2: Salicylic acid (a) and 2,3-dihydroxy benzoic acid (b) production by *Rhizobium* OS1 at varying concentration of MONPs

ISSN: 0976-3104
REGULAR ISSUE
Amara

THE IIOAB JOURNAL

RESEARCH ARTICLE OPEN ACCESS

PROTEASES AND THEIR ADAPTATION

Amro Abd Al Fattah Amara[1]*

[1]*Prof. Department of Protein Research, Genetic Engineering and Biotechnology Research Institute, City for Scientific Research and Technology Applications, Universities and Research Centre District, New Borg El-Arab, P.O. Box 21934, Alexandria, EGYPT*

ABSTRACT

The amino acids constituents of the various proteins play a crucial role in their structures/functions. The proteases variations are well explained due to their differences in their of amino acids constituents. However, such differences are not explained at DNA level. But, it is assumed that, at DNA level, much variation could be seen and many factors could be responsible for such differences. However, which factor(s) could affect more than the other are not yet elucidated. One factor could be the differences in environmental conditions, because the thermophilic proteases are existed in thermophilic environment, but mesophilic ones existed in their favorite habitat. Such genetic changes and subsequent changes in polypeptide chains are due to the environmental adaptation. Here, proteases coding twelve DNAs (nucleotides) and their translated products (amino acids) from different microbes adopted in different environmental conditions were analyzed using a combined bioinformatics approach. The results show that, there is a clear correlation between the nucleotides and amino acid constituents of different proteases therefore, proving a link between the microbes' types and environments they are adopted in. This study opens a new window and warrens to give equal attention to DNA in understanding the adaptation of microbes in various environmental conditions

Received on: 02nd-April-2012
Revised on: 07th-May-2012
Accepted on: 25th– Apr-2012
Published on: 8th –May-2012

KEY WORDS

Nucleotides, Amino acids, Protease, Protein Model, Comparative analysis

***Corresponding author:** Email: amroamara@web.de Tel: +00201010777905; Fax: +2034593423

[I] INTRODUCTION

The diversity is a common criterion within microbes [1]. Such diversity gives each microbe a fingerprint, which makes it different somehow from the other ones [2]. Within the same species there is a big level of diversity can be found particularly within strains existed in different habitats [3]. This is mainly because of unicellular microbes reflect clearly any genetic variation, while they follow mostly the role of "Single cell with single copy of each gene; gives a single protein". That protein gives (mostly) single function [1, 4]. Unicellular microbes have different routes of gaining new genes including, transformation, transduction, hyperdization, transposones elements, phage infections and mutations [5]. As an example, which could explain the dynamics of gene transfer, β-lactamase is given [1]. Another example is the enterohemorrhagic *E. coli* isolates containing virulence plasmids and pathogenicity islands similar to those found in *Shigella spp* [6]. In higher genera; chromosomal recombination, mitosis and sexual reproduction are other sources of variation. Lower, microbes could also do DNA recombination when big DNA part (might be transferred from dead microbes) or homologues DNA fragment inter to the cytoplasm and find a place (with special sequence) to do recombination. The elevation of the antibiotic resistance in sensitive microbes is a clear example. [1, 6]. Microbial resistance teaches us that microbes have uncommon ability to survive depending on one of the mechanisms of the different types of gene(s) transformation. The DNA is the code for the protein, which mediated through the synthesis of intermediate macromolecules, the RNA. Changes in the DNA will be reflected on the protein and will be affecting on its original structure/functions. Mutagenesis, (particularly the site directed mutagenesis), the protein engineering and the enzyme activity (and many others) prove that [7, 8]. The different DNA and protein databases could add some points to such prove further, such as changes in the DNA and protein sequences. Particularly the differences within the same type (class) of enzyme on the strain level within a certain species will be more interesting. Because, such differences will be able to reflect the role of both of the amino acids and the nucleotides. The protein primary structure, could explain the structures/functions, because it is the main macromolecules, which do the function. However, the DNA can be also an interesting subject for investigating such variation within the same class or within different classes [9]. That because, two similar proteins did not mean two similar genes. Therefore, regarding the diversity, the DNA will be the best choice for detecting minor variation. However, study the DNA variation due to different functions or adaptation was neglected particularly if one relating such variation in protein functions to their environmental adaptation. Alternatively, this study investigates if there is a relation between the DNA protection (from any unusual conditions such as the environmental

conditions) and the protein behavior. In this study I try to put a spot on the DNA as an element, could side by side with its protein explain the variation within similar proteins and different function as a result for different environmental and adaptation factors.

[II] MATERIALS AND METHODS

2.1. The used protein and DNA sequences

Twelve protein and DNA sequences have been collected from BLAST (NIH) database and represent: (1) *Bacillus sp*. L010 serine alkaline mesophilic protease precursor (sprD) KC153302.1 [10]; (2) Uncultured bacterium protease for serine mesophilic protease (Antarctic costal sediment) FM163400.1 [11]; (3) *Pseudoalteromonas sp*. SM9913 cold-adapted halophilic subtilase serine protease IFO 3455 (AP) (deep-sea psychrotolerant bacterium) MCP-03 [12]; (4) *Pseudomonas aeruginosa* mesophilic alkaline metalloprotein proteinase-D87921.1 [13]; (5) *Flavobacterium indicum* GPTSA100.9 (hot spring water) [14]; (6) Antarctic psychrotroph *B. subtilis* (TA41) sub gene for subtilisin-X63533.1 [15]; (7) AY028615. 1 *Bacillus* (*Geobacillus*) *stearothermophilus* thermophilic alkaline protease [16]; (8) *B. sp*. Subtilisin-like thermophilic serine SG-1-1101501000595 [17]; (9) U31759. 1 *Thermoactinomyces sp*. thermostable alkaline protease [18]; (10) HM192828. 1 *Laceyella sacchari* strain DSM 43353 thermitase [19]; (11) *Bacillus thuringiensis str*. Thermitase Al Hakam chromosome [20]; (12) *Thermosipho africanus* TCF52B-NC_011653.1 serine protease MucD [21]. The GeneBank or the NCBI Reference sequence for each protease and its producing microbes are: GenBank: AY028615.1 *Bacillus stearothermophilus*| GenBank: KC153302.1 *Bacillus sp*. L010| GenBank: FM163400.1 Uncultured bacterium| GenBank: DQ422814.1 *Pseudoalteromonas sp*.| GenBank: D87921.1 *Pseudomonas aeruginosa* |GenBank: X63533.1 *B. subtilis* | GenBank: ABCF01000018.1 *Bacillus sp* | GenBank: U31759.1 *Thermoactinomyces sp*.| GenBank: HM192828.1 *Laceyella sacchari*| NCBI Reference Sequence: YP_005356102.1 *Flavobacterium indicum* | NCBI Reference Sequence: NC_008600.1 *Bacillus thuringiensis* str. Al Hakam| NCBI Reference Sequence: NC_011653.1 *Thermosipho africanus*.

The amino acids and nucleotides sequences of those strains can be found in the amino acids and the nucleotides alignment in this study. The amino acids and the DNA sequences are adjusted to FASTA format to enable various types of analysis using the different software used in this study [22-25].

2.2. The software used in this study

Several software were used in this study to do various proteins' and DNAs' amino acids and nucleotides sequences analysis. Clustal W v. 1.7 was used to alignment both of the amino acids and the nucleotides used in this study **[Figures– 1,4]** and to generate BOOTSTRAP N-J tree **[Figures–3a,3c]**. FigTree v.1.4 was used to visualize the trees obtained from the amino acids and the nucleotides alignments **[Figure–3a, 3c]**. PAST statistical package was used to do clustering for the different numeric data **[Figures – 3b,3d]**. MEGA v. 5.1 was used to generate comparative analysis for the twelve amino acids sequences as in **Table–1** and **Figure–2**. BioEdit v.7.1.11 was used for the analysis of the nucleotides compositions as in Table 2. MODELLER 9v8 was used in protein models generation for the twelve amino acids sequences used in this study **[Figure – 5]** against six published protease models. And for calculating the % of similarity of each protein sequence with the six used models as in **Table 3 [26-33]**.

2.3. Generating amino acids profiles

For each of the twelve different proteins of the proteases enzymes, an amino acids profile was generated **[Table – 1]**. For each profile, each amino acid has been given as % and the overall data has been summarized in **Table– 3**. For that the software OMGA 5.1 was used to analyze the sequences collected for each protein individually and for all of the twelve used sequences collectively. An average for each of the twenty amino acids for the twelve sequences have been also calculated and given as an average %. OMGA 5.1 enables calculating the % of each amino acid in each protein. The average of each amino acid % for each the twelve proteins was summarized in **Table– 1**.

Commented [D1]: No Result section, No caption for Fig 2

2.4. Allignment and phylogenic trees

Alignments and Phylogenic trees for the proteins primer sequences of amino acids and nucleotides have been generated **(Figure – 1, 4)**. The sequences alignment and the phylogenic trees have been generated using Clustal W version 1.7. The software does alignment for both of the amino acids and the nucleotides used in this study and generate a BOOTSTRAP N-J tree for each. FigTree v1.4 has been used to visualize the trees obtained from both of the alignment of the different proteins' amino acids and nucleotides **(Figure –3a, 3c)**.

2.5. Generating proteases protein models

A model for each of the twelve proteases has been generated using the software MODELLER v 9.8 **[Figure– 5]**. Six published protease models have been used to build the hypothetical model for each of the twelve proteases using MODELLER v 9.8. against six published protease models represent 2GKO (S41 *Psychrophilic subtilisin* (x-ray) [34], 2IXT S41 *Psychrophilic subtilisin* (x ray) [35], 1O0T Cold-adapted alkaline psychrophilic metalloprotease (x-ray) [36], 2PEF Mesophilic protease A (x-ray) [37] 1DBI Thermostable serine protease (x-ray) [38] , and 1SNG Thermophilic serpin in native state (x-ray) [39] models. An overall alignment for the twelve generated models has been generated as in **Figure–6**.

Because the proteases are related to microbes from different environmental conditions they are different from each other. The proteases investigated in this study represent cold-adapted, mesophilic, thermophilic, thermitase, metalloprotease, alkaline, serine, endopeptidases, subtilisine and subtilisine like. For any protein, the 3D structure plus the chemical and physical conditions (where it existed) determined and control the protein structures/functions. However, the 3D structure is depending on the primary structure of the protein. In other word, the protein 3D structure depend on its constituents of amino acids. In addition, the constituent of the amino acids is depending on the DNA nucleotides sequences. For that, both of the proteins' amino acids and nucleotides sequences were investigated in this study to enable better understanding for any variation could be linked to the amino acids and the nucleotides primary structure; the protein structures/functions as well as the protein physical adaptation. The amino acids alignment and the phylogenetic tree show that there are clustering for the thermophilic proteases as well as for the mesophilic proteases **[Figure– 1, 3]**. The same results could be obtained from the nucleotides analysis as in **Figure–3, 4**. The amino acids distributions within the twelve tested protein which were

IIOAB JOURNAL
ISSN: 0976-3104

determined using MEGA 5.1 software were summarized in **Table–1** and **Figure– 2**. Cys is represented in the lesser percentage. That might be explained; that proteases did not need any sort of rigidity or within molecules sulfur bonds, which is a characteristic future for the Cys. The amino acids constituents of the twelve investigated proteases could be ranked from the lower to the higher % as in **Table– 1**. Cys was the lowest one according to its % and followed by Trp, His, Met, Arg, Phe, Glu, Gln, Pro, Tyr, Ile, Leu, Asp, Lys, Thr, Asn, Val, Ser, Gly and Ala. Serine which is an important residue in the proteases active site was ranked a number eighteen. That may explain the presence of protease activity even after the fragmentation of the enzyme as suggested by Amara et al 2013 [41]. The analysis also spot the homogeneity regarding to the amino acids constituent between the investigated proteases. Only *Pseudomonas aeruginosa* has remarkable number of amino acids different from the other compared strains as in **Figure– 2**. That might explained the role of the biofilm formation by *Pseudomonas aeruginosa*, its survive, under certain conditions enable the death of other microbe(s) and the possibility of its acquiring DNA fragments from such microbes [5]. Some strains have minor differences (e.g. *Laceyella sacchari*). Proteases for such unique constituents of amino acids are fast folded and fast interact with their substrate. They could reach their optimum activities in seconds. The nucleotides sequences analysis, which was conducted by BioEdit v. 7.1.11 to calculate each of GC percentage, AT percentage, Molecular weight of single and duple strand and used the number of each of A, T, G and C nucleotides. The cluster analysis for the amino acids percentage data in **Table–1** and which obtained from the PAST statistical package software could better summarize the data in **Table–1**. The cluster put amino acids with similar percentage in groups near each other based on the similarity. As well as it put microbes similar in their amino acids profile in groups. The same was done for the nucleotides sequences in **Table– 2** as well as the GC percentage and AT percentage in **table– 2** and **Figure– 3.** There are minor differences could be found in the three clusters mediated by PAST software in **Figure – 3** and generated from the data in **Table– 1, 2**. This increase the chance of the DNA to be more observed in the future research. From the **Figure– 3** thermophilic proteases as well as the nonthermophilic ones are clustered to similar groups. This might not be clearly distinguished from the protein 3D alignment for the proteases models. For the twelve amino acids sequence, twelve protein models were generated. The models were generated against six resolved and published proteases models [34-39]. The template models represent three thrmophilic, one mesophilic, one psychrophilic and one cold-adapted alkaline protease. For more details, refer to references numbers [34-39]. The three dimensional structure of the different models apparently are similar. Most of them give similar total configuration but with differences in some of their chains, mainly represented in shorter or longer chain if compared with other ones **[Figure– 4]**. The alignment for the all proves that they could be fitted somehow to one alignment model as in **Figure–5**. Interestingly the % of similarity between them and between the six template models are ranging from 11% to 19%. Only one odd protease gives 47.6% of similarity [*B. subtilis* as in **Table– 3**]. The protease of Pseudoalteromonas model gives % of similarity bigger than the four other models **[Table–3]**. Pseudoalteromonas protease model expected to give the smallest % of similarity because its molecular weight is nearly 1.5 bigger than the other proteases. In general, the 3D structures of the proteases even are similar but still able to give some valuable information. Enzymes are used in different kind of medicinal and technical applications [42]. They are protein in nature. Their function can be determined against different substrates as unit of activity [42]. They are sequences of amino acids. And have a DNA codes. The variation between them for that is mainly due to the variation in their nucleotides. In the age of the protein engineering there is a real need for doing more comparative analysis to understand what going on, and what are the player in determining the protein structures/functions [42]. In the EMBO conference for Comparative genomic of Eukaryotic microorganisms (2009) Spain Amara et al introduce the importance of the collective amino acids constituents in the PhaC synthases different classes functions and that similar classes have some similarity in their amino acids constituents, particularly the conserved amino acids residue [43-45]. In fact, such observation has come out from the random mutagenesis study published in 2002 and conducted during 1999 to 2002 for three years on the PhaC synthases classes I and II aiming to change their substrate specificity from one to another [46]. This study leads to determining enhanced PhaC enzyme activity mutants with minor change in the produced polymers' monomeric constituents with minor change in the substrate specificity and enhancement in the enzymes activities [47]. Amino acids in places other than the catalytic residue are responsible for such enzyme activity enhancement. The amino acids collectively for the different enzymes related to classes of PhaC were also analyzed [43-45]. This differences have somehow significant roles in the minor changes within the same type of enzyme in a particular class and lead to the clear variation within the different classes [46]. In fact there are many scientific work discuss the similarity between the amino acids within related enzymes. However, lesser who have been attracted to study differences within nucleotides and related such differences to function or adaptation. This study furthermore attract the attention that, differences within the same protein from a DNA point of view could be also a good guide for understanding the protein structure function. Particularly, if the protein and the DNA differences are due to environmental conditions. DNA phylogenic tree show more variation than the amino acids tree does. Not only, such differences might be due to strain diversity, but also it might due environmental adaptation. In simpler words, I suggest that there might be some built in tools and mechanisms in each microbe induce changes in the DNA to adapt certain environmental conditions firstly and to adjust the produced protein itself. Epigenetic teach us that such possibility could

be happened [48, 49]. Such changes might have a controlled mechanisms and its machinery. As an example the spore formation is, considers a great change happened in the microbe structure and controlled by genes and proteins inside its genome [50]. This will lead us to a conclusion that, we have a very little information about the mechanisms govern the changes happened due to external inducer. This might be due to internal mechanism enable such changes and not due to what is commonly known as mutation. It might be certain similar structures and elements govern the microbes' adaptation, which we still did not know.

[IV] CONCLUTION

This study simply targeted twelve proteins and their DNA sequences to map, similarity, differences, conduct various molecular and bioinformatics analysis and do a logical analysis for both of the similarities and differences and to correlate that to the environmental conditions where the protein is work based on its properties (alkaline, thermophilic, serine, cold-adapted, psychlotrophic, thermophilic, mesophilic etc). For that different software could do different analysis have been used. Mainly to do alignment, phylogenic tree and similarity analysis, building protein models, calculating the nucleotides and the amino acids constituents and do comparative analysis for both of them as well as calculating the GC, and AT%. For starting such work, both of the amino acids and nucleotides sequences of the twelve protein (which have various properties and represent different bacterial strains live in different ecological systems and habitat) and DNA sequences have been collected from the NIH BLAST database. Clustal W v. 1.7, have been used to do the different analysis as described in details in the MMs section. The sequences have adjusted to a FASTA format for analysis. Six well identified and published proteases models have been used for building the various proteases models. The protein models could not explain clearly the differences in the protein functions alone. However, one point could be highlighted here that some of the dissimilarity in the different protein 3D structure are due to the length of the amino acids sequences, of course and the differences in the amino acid constituents. Each microbe has been created to adapt certain conditions. The different phylogenetic trees and cluster analysis for the data in this study prove that proteases with similar environmental conditions cluster together in similar chains. The phylogenic trees prove that DNA sequences could be used in the understanding of the protein type of adaptation while similar proteins clustered near to each other in most case. The data from the protein models in Figure 1 and the alignment between all proteins prove the similarity. DNA analysis if related to the protein physical conditions or functions could also explain the type of changes happened due to different habitat, activity, physical and chemical conditions..

CONFLICT OF INTEREST

The authors have no conflict of interests to declare.

FINANCIAL DISCLOSURE

Institutional support

ACKNOWLEDGEMENT

The author acknowledges the City of Scientific Research and Technological Applications for supporting this work.

REFERENCES

[1] Amara AA, Shibl AM, Tawfik AF. [2012] Deeper in the antibiotics paradigm: Microbes react individually and collectively for spreading the resistance," *African Journal of Microbiology Research* vol. 6(9): 2010v2019,

[2] Blattner FR, Plunkett G, Bloch CA. et al. [1997] The complete genome sequence of *Escherichia coli* K-12, *Science* 277: 1453–1474.

[3] G. De La Cueva-Méndez and B. [2007]bPimentel "Gene and cell survival: lessons from prokaryotic plasmid R1," *EMBO. Report*, 8(5): 458–464

[4] Mendoza Mdel C, Herrero A, Rodicio MR [2009] [Evolutionary engineering in Salmonella: mergence of hybrid virulence-resistance plasmids in non-typhoid serotypes]. Enferm. Infect. *Microbiol Clin* 7(1): 37–43.

[5] Amara, AA. [2011] Opportunistic pathogens and their biofilm "food for thought" In Science against microbial pathogens: Communicating current research and technology advances: Edit by Mendez-Vilas. FORMATEX Microbiology Series No 3 Vol 2: 813–824.

[6] Makino K, Ishii K, Yasunaga T, et al. [1998] Complete nucleotide sequences of 93-kb and 3.3-kb plasmids of an enterohemorrhagic *Escherichia coli* O157:H7 derived from Sakai outbreak. *DNA Res* 5: 1–9

[7] Hutchison CA, Phillips S, Edgell MH. Et al. [1978]. Mutagenesis at a specific position in a DNA sequence. *J Biol Chem* 253(18): 6551– 6560.

[8] Winter G, Fersht AR, Wilkinson AJ, et al. [1982] Redesigning enzyme structure by site directed mutagenesis: Tyrosyl tRNA synthetase and ATP binding. *Nature* 299(5885): 756–758.

[9] Satyanarayana T, Raghukumar C, Shivaji S. [2005] Extremophilic microbes: Diversity and perspectives. *Current Science* 89(1): 78–90

[10] Li D, Huang F, Jiang Y. et al. [2012] Molecular cloning and expression of a novel mesophilic protease from Bacillus sp. L010 in *Escherichia coli* Unpublished Direct Submission (11-NOV-2012) *College of Life Sciences*, Sichuan

[11] Zhang Y, Zhao J, Zeng,R. [2011] Expression and characterization of a novel mesophilic protease from metagenomic library derived from Antarctic coastal sediment *JOURNAL Extremophiles* 15 (1): 23–29

[12] Yan,BQ, Chen XL, Hou XY. [2009] Molecular analysis of the gene encoding a cold-adapted halophilic subtilase from deep-sea psychrotolerant bacterium Pseudoalteromonas sp. SM9913: cloning, expression, characterization and function analysis of the C-terminal PPC domains *JOURNAL Extremophiles* 13 (4):725–733

[13] Okuda K., Morihara K., Atsumi Y. et al. [1990] Complete nucleotide sequence of the structural gene for alkaline proteinase from Pseudomonas aeruginosa IFO 3455 *JOURNAL Infect. Immun* 58 (12): 4083–4088

[14] Barbier P, Houel A, Loux V, et al. [2012] Complete genome sequence of Flavobacterium indicum GPSTA100-9T, isolated from warm spring water *J Bacteriol* 194 (11):3024–3025
[15] Davail S, Feller G, Narinx E. et al. [1992] TITLE Sequence of the subtilisin-encoding gene from an Antarctic psychrotroph Bacillus TA41 JOURNAL Gene 119 (1), 143-144 (1992) Bacillus sp. SG-1 1101501000595, whole genome shotgun sequence
[16] Fu Z, Hamid SB, Razak CN. [2003] Basri,M., Salleh,A.B. and Rahman,R.N.Secretory expression in Escherichia coli and single-step purification of a heat-stable alkaline protease *Protein Expr. Purif* 28 (1):63–68
[17] Tebo B, Ferriera S, Johnson J. et al. [2007] Direct Submission (08-JUN-2007) J Craig Venter Institute, 9704 Medical Center Drive, Rockville, MD 20850, USA
[18] Lee JK, KimYO, Kim HK., et al. [1996] Purification and characterization of a thermostable alkaline protease from Thermoactinomyces sp. E79 and the DNA sequence of the encoding gene *Biosci. Biotechnol. Biochem* 60 (5): 840–846
[19] Jorgensen CM, Madsen SM, Hansen OC et al. [2010] TITLE Original-like thermitase from Laceyella and its safe heterologous expression Direct Submission (06-MAY-2010) Bioneer a/s, Kogle Alle 2, Horsholm DK-2970, Denmark
[20] Challacombe JF, Altherr MR, Xie G, et al.[2007] The complete genome sequence of Bacillus thuringiensis *Al Hakam JOURNAL J Bacteriol* 189 (9):3680–3681
[21] Nesbo,C.L., Bapteste,E., Curtis,B., et al. [2009] The genome of Thermosipho africanus TCF52B: lateral genetic connections to the Firmicutes and *Archaea J Bacteriol* 191 (6): 1974–1978
[22] Altschul SF, Gish W, Miller W. et al. [1990] Basic Local Alignment Search Tool. *J Mol Biol* 215:403–410.
[23] Altschul SF, Madden TL, Schaffer AA, et al. [1997] Gapped BLAST and PSI-BLAST: a new generation of protein database search programs. *Nucleic Acids Res* 25:3389–3402.
[24] Madden T. [2002] The BLAST Sequence Analysis Tool. 2002 Oct 9 [Updated 2003 Aug 13]. In: McEntyre J, Ostell J, editors. The NCBI Handbook [Internet]. Bethesda (MD): National Center for Biotechnology Information (US); 2002-. Chapter 16. Available from: http://www.ncbi.nlm.nih.gov/books/NBK21097/
[25] Tao Tao. [2011] "Single Letter Codes for Nucleotides". NCBI Learning Center. National Center for Biotechnology Information. Retrieved 2012-03-15. "IUPAC code table". NIAS DNA Bank.
[26] Tamura K, Peterson D, Peterson N, et al. [2011] MEGA5: Molecular Evolutionary Genetics Analysis using Maximum Likelihood, Evolutionary Distance, and Maximum Parsimony Methods. *Mol Biol Evol* 28: 2731–2739
[27] Thompson JD, Higgins DG, Gibson TJ. [1994] CLUSTAL W: improving the sensitivity of progressive multiple sequence alignment through sequence weighting, position-speci?c gap penalties and weight matrix choice. *Nucleic Acids Research* 22: 4673–4680.
[28] Rambaut A. [2012] Figtree v 131, http:// tree.bio.ed.ac.uk/software/figtree 12.05-v 1.4
[29] Hall TA. [1999] BioEdit: a user-friendly biological sequence alignment editor and analysis program for Windows 95/98/NT. *Nucl Acids Symp Ser* 41: 95-98.
[30] Felsenstein J. [1992] Estimating effective population size from samples of sequences: a bootstrap Monte Carlo integration method. *Genet Res* 60(3):209–220.
[31] Allerberger F [2003] Listeria: growth, phenotypic differentiation and molecular microbiology. FEMS. *Immunol. Med. Microbiol* 35(3): 183–189.
[32] MA Marti-Renom, A Stuart, A Fiser, R Sanchez, et al.[2000] Comparative protein structure modeling of genes and genomes. *Annu. Rev. Biophys. Biomol. Struct*. 29: 291–325
[33] Hammer Ø, Harper DAT, Ryan PD. [2001] PAST: Palaeontological statistics software package for education and data analysis. *Palaeontologia Electronica* 4(1):http://palaeoelectronica.org/2001_1/past/issue1_01.htm
[34] Walter RL, Mekel MJ, Grayling RA, et al. [2009] The crystal structures of the psychrophilic subtilisin S41 and the mesophilic subtilisin Sph reveal the same calcium-loaded state. *Proteins* 74: 489–496
[35] Almog O, Gonzalez A, Godin N.[2009] The Crystal Structures of the Psychrophilic Subtilisin S41 and the Mesophilic Subtilisin Sph Reveal the Same Calcium-Loaded State. *Proteins* 74: 489
[36] Ravaud S, Gouet P, Haser R et al. [2003] Probing the role of divalent metal ions in a bacterial psychrophilic metalloprotease: binding studies of an enzyme in the crystalline state by x-ray crystallography. *J Bacteriol* 185: 4195–4203
[37] Kelch BA, Agard DA. [2007] Mesophile versus Thermophile: Insights Into the Structural Mechanisms of Kinetic Stability *J Mol.Biol* 370: 784–795
[38] Smith CA, Toogood HS, Baker HM, et al. [1999] Calcium-mediated thermostability in the subtilisin superfamily: the crystal atructure of Bacillus AK.1 protease at 1.8 a resolution. *J MOL BIO* 294:1027–1040
[39] Fulton KF, Buckle AM, Cabrita LD, et al. [2005] The high resolution crystal structure of a native thermostable serpin reveals the complex mechanism underpinning the stressed to relaxed transition. *J Biol Chemb*280 : 8435–8442
[40] Feng DF, Doolittle RF. [1987] Progressive sequence alignment as a prerequisite to correct phylogenetic trees. *J Mol Evol* 25: 351–360.
[41] Amara AA, Younis AMM, Salem SR Shabeb MSA. [2013] Mixed enzymes show enhanced activities. *International Science and Investigation Journal* 1–11
[42] Amara AA. [2013] Pharmaceutical and Industrial protein engineering: Where we are? PJPS. 217–232
[43] AA Amara, SM Matar, E Serour. [2012] comparative amino acids studies on PhaC synthases and proteases as well as establishing a new trend in experimental design. IIUM *Engineering Journal* Vol. 13 No. 1, 35–47
[44] E Serour, AA Amara, MS Matar. [2009]"Comparative study between thermophilic and mesophilic lipases and proteases". EMBO –Conference- "Comparative genomics of Eukaryotic microorganisms" 77
[45] S Mater, AA Amara, E Serour. [2009] "Study the possibility of lipases overproduction using media constituents designed based on genomic comparative

study". EMBO –Conference "Comparative genomics of Eukaryotic
[46] AA Amara, MS Matar E Serour. [2009]"Comparative study on the amino acids constituents of PhaC synthases Class I, II, III and IV" EMBO –Conference- "Comparative genomics of Eukaryotic microorganisms" 59: 2009
[47] A A, Steinbüchel A, Rehm BHA. [2002] In vivo evolution of the Aeromonas punctata polyhydroxyalkanoate (PHA) synthase: Isolation and characterization of modified PHA synthases with enhanced activity. *Appl. Microbiol. Biotechnol* 59:477–482
[48] Proceedings of the First Russian-European Workshop on DNA Repair and Epigenetic Regulation of Genome Stability. St. Petersburg, Russia. Dedicated to the Memory of Nikolay Tomilin. *Mutat. Res.* [2008] 685: 1–102.
[49] Egger G, Liang G, Aparicio A et al. [2004] Epigenetics in human disease and prospects for epigenetic therapy. *Nature* 429(6990), 457–463.
[50] Errington J. [2003] Regulation of endospore formation in Bacillus subtilis. *Nature reviews* 1:117–126

ABOUT AUTHOR

*Prof. **AMRO ABD-AL-FATTAH AMARA** is working in the field of molecular microbiology and, biotechnology. He is the Head of the protein research department in (Mubarak) City for scientific research and, technological applications. He is interested in linking science to the real life to find simple solutions for problems could be costly for many.*

IIOAB JOURNAL
ISSN: 0976-3104

Supplementary Materials (As supplied by author)

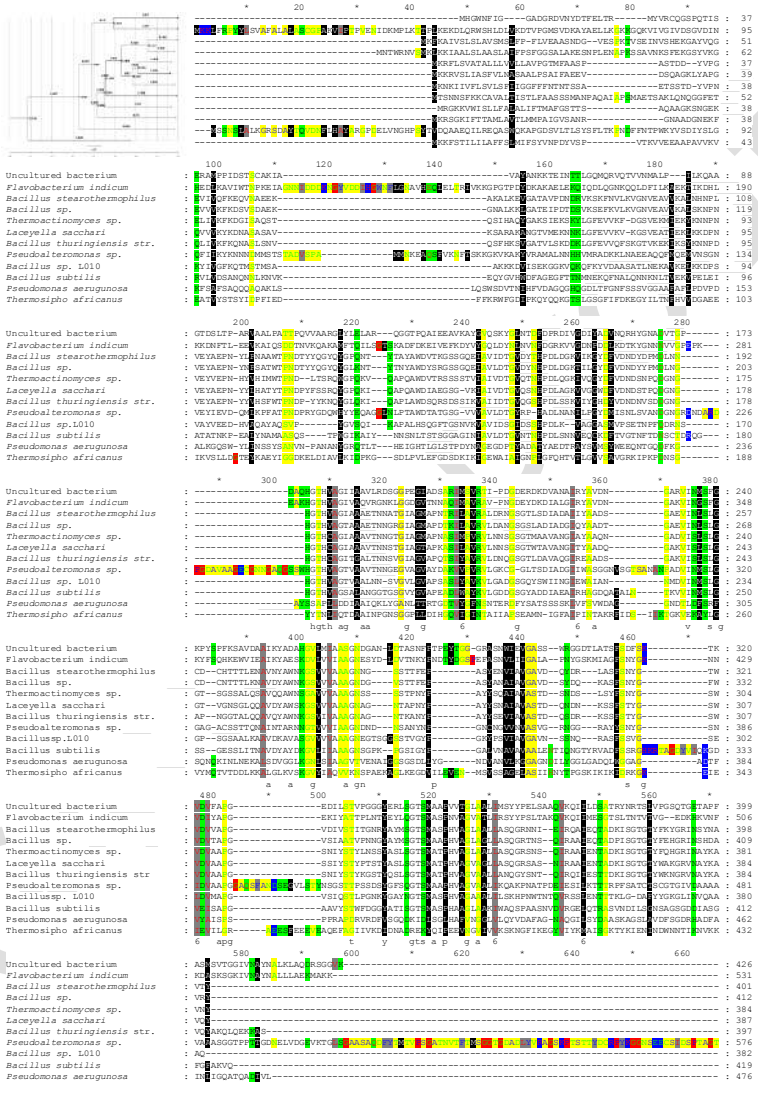

Supplementary fig. 1: Multiple alignment of the primary sequences of twelve proteases' amino acids.

IIOAB JOURNAL
ISSN: 0976-3104

Supplementary table: 1. Proteases different amino acids % and an average for each amino acid of the twelve tested proteases.

Protease bacterial host	Amino acids %																				
	Cys	Trp	His	Met	Arg	Phe	Glu	Gln	Pro	Tyr	Ile	Leu	Asp	Lys	Thr	Asn	Val	Ser	Gly	Ala	Total
B. subtilis Antarctic psychrotroph	0.5	1.2	1.7	1.9	2.4	2.6	3.6	3.1	2.9	3.1	5	5.5	5.7	4.5	6.9	8.6	7.4	8.1	11.5	13.8	419
Pseudoalteromonas sp. Serine/cold adapted/halophilic subtilase	1.6	0.8	1.4	2.7	2.1	2.5	2.7	3.4	4.4	3.8	3	3.9	5.4	3.7	9	8.2	7.3	9.6	12.1	12.4	709
Uncultured bacterium Serine mesophilic	0.5	0.7	1.2	2.6	5.2	2.3	3.3	3.8	5.2	4	5.6	5.4	6.8	3.5	7.3	4.2	7.7	7.3	10.3	13.1	426
Bacillus sp. L010 Serine/alkaline/mesophilic	0	1	1.8	2.4	1	2.4	2.9	3.9	3.7	3.4	4.2	5.5	3.4	7.3	5	5.2	10.5	11.8	10.7	13.9	382
Pseudomonas aeruginosa Alkaline/mesophilic	0	1.5	1.7	0.4	2.5	4.8	2.3	5.3	3.2	4.8	3.6	8.8	8.4	3.4	5.3	6.1	5.7	10.3	10.5	11.6	476
Flavobacterium indicum Hot spring subtilisin/thermophilic	0.2	0.8	1.7	1.7	1.5	2.6	5.1	3.4	4	4.7	6.2	7.3	8.1	11.1	5.1	7.2	8.5	4.5	7.9	8.5	531
Bacillus sp. Serine/subtilisine-like/thermophilic	0.5	1.2	1.5	1.5	1.9	2.7	3.9	1.9	3.6	5.6	3.9	5.8	6.6	5.8	6.6	7.5	8.3	8.5	9.5	13.3	412
Thermoactinomyces sp. Alkaline/thermophilic	0.3	1.3	2.1	2.1	1.8	2.1	2.1	4.9	4.2	4.9	5.2	5.2	4.4	3.6	6	7	8.6	12.2	8.9	13	384
Laceyella sacchari Thermitase	0.3	1.6	1.3	0.8	1.8	1.6	2.6	3.6	4.1	5.2	4.4	4.1	4.4	6.2	6.5	6.7	9.3	10.3	9.8	15.5	387
Bacillus thuringiensis Thermitase	0.3	1.3	1.8	0.5	1.5	2.8	2.3	5.8	3	5.8	5.8	4.8	5.3	6.8	6.5	6.8	8.6	11.6	8.8	10.1	397
Thermosipho africanus Thermitase	0	0.7	0.9	1.3	1.3	4.9	7.5	2.2	3.8	5.1	11.5	5.3	5.7	9.9	4.4	4.6	8.6	6	9.3	7.1	453
Bacillus stearothermophilus Alkaline/thermophilic	0.5	1	1.7	1.5	2.2	2.5	5	2.7	3.2	5.7	5.2	5.2	6	4.5	6.7	8	10.2	7	8.2	12.7	401
Average	0.4	1.1	1.5	1.7	2.1	2.8	3.6	3.6	3.8	4.6	5.2	5.6	5.9	5.9	6.4	6.8	8.3	8.8	9.9	12	448.1

Supplementary table: 2. Proteases different nucleotides analysis

Protease bacterial host	G+C content	A+T content	Length/base pairs	Molecular Weight Daltons, single [illegible]	Molecular Weight Daltons, double stranded	Number A	Mol% A	Number T	Mol% T	Number C	Mol% C	Number G	Mol% G
B. subtilis Antarctic psychrotroph	48.10%	51.90%	1260	382866	765582	370	29.37	284	22.54	278	22.06	328	26.03
Pseudoalteromonas sp. Serine/cold adapted/halophilic subtilase	47.19%	52.81%	1689	511701	1025972	453	26.82	439	25.99	362	21.43	435	25.75
Uncultured bacterium SERINE MESOPHILIC	61.36%	38.64%	1281	389902	781229	275	21.47	220	17.17	358	27.95	428	33.41
Bacillus sp. L010 Serine/alkaline/mesophilic	51.21%	48.79%	828	251994	503548	206	24.88	198	23.91	215	25.97	209	25.24
Pseudomonas aeruginosa Alkaline/mesophilic	63.45%	36.55%	1431	438054	873213	281	19.64	242	16.91	478	33.4	430	30.05
Flavobacterium indicum Hot spring subtilisin/thermophilic	34.27%	65.73%	1596	482786	965977	442	27.69	607	38.03	320	20.05	227	14.22
Bacillus sp. Serine/subtilisine-like/thermophilic	44.87%	55.13%	1239	375180	752145	293	23.65	390	31.48	286	23.08	270	21.79
Thermoactinomyces sp. Alkaline/thermophilic	52.29%	47.71%	1155	352988	702611	306	26.49	245	21.21	325	28.14	279	24.16
Laceyella sacchari Thermitase	55.24%	44.76%	1164	356707	708669	289	24.83	232	19.93	363	31.19	280	24.05
Bacillus thuringiensis Thermitase	36.77%	63.23%	1194	361759	723183	361	30.23	394	33	234	19.6	205	17.17
Thermosipho africanus Thermitase	32.16%	67.84%	1362	413362	823864	412	30.25	512	37.59	286	21	152	11.16
Bacillus stearothermophilus Alkaline/thermophilic	41.21%	58.79%	1206	365508	731361	382	31.67	327	27.11	227	18.82	270	22.39

IIOAB JOURNAL
ISSN: 0976-3104

Supplementary table: 3. Different Proteins similarity % to the 1D0T, 1SNG, 2GKO, 2IXT and 2PEF models

Protease bacterial host names	Similarity % to the used cited six models [10-21]	Rank
B. subtilis	47.573	1
Laceyella sacchari	19.188	2
Thermoactinomyces sp	18.450	3
Uncultured bacterium	18.122	4
Bacillus stearothermophilus	18.080	5
Bacillus sp	17.712	6
Bacillus thuringiensis	15.858	7
Pseudoalteromonas sp	13.916	8
Flavobacterium indicum	13.226	9
Bacillus sp. L010	12.903	10
Thermosipho africanus	12.258	11
Pseudomonas aeruginosa	11.327	12

Supplementary figure: 2. Proteases different amino acids %

IIOAB JOURNAL
ISSN: 0976-3104

Supplementary figure: 3. Phylogenic trees and cluster for each of. 3a) amino acids sequences; 3b) nucleotides sequences (The branching order and distance score were calculated by the program tree as described by Feng and Doolittle (1987) [40]; The trees have been visualized using FigTree v. 1.4.); 3b) Cluster analysis for the amino acids 3d) nucleotides constitents; 3e) GC% and AT% nucleotides constitents. Generated using PAST software using Paird group algorithm (two way with constraind) in the cluster analysis option.

Supplementary figure: 3a

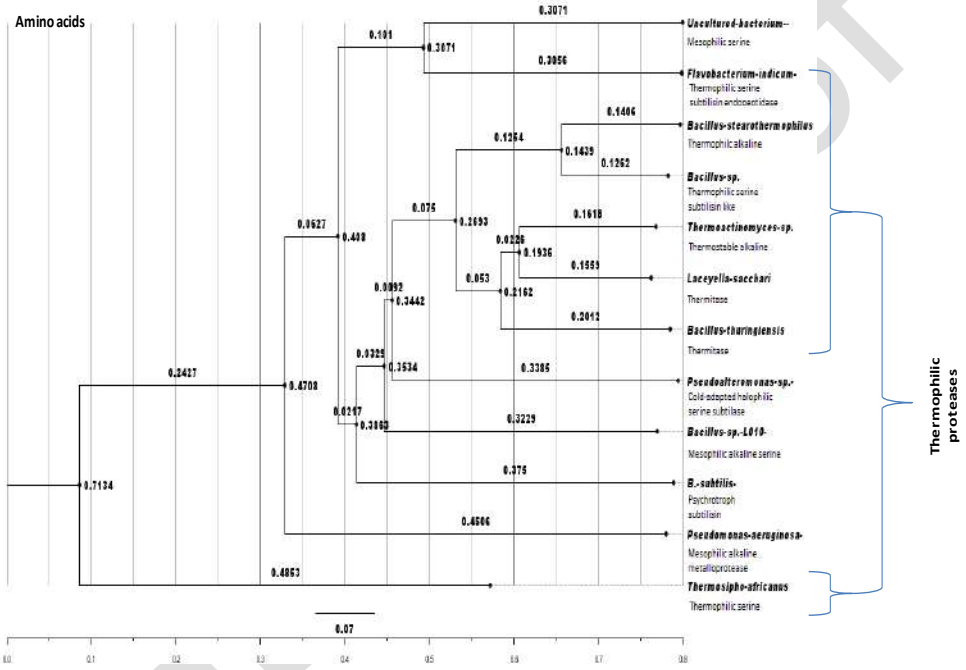

CHEMISTRY

IIOAB JOURNAL
ISSN: 0976-3104

Supplementary figure: 3b.

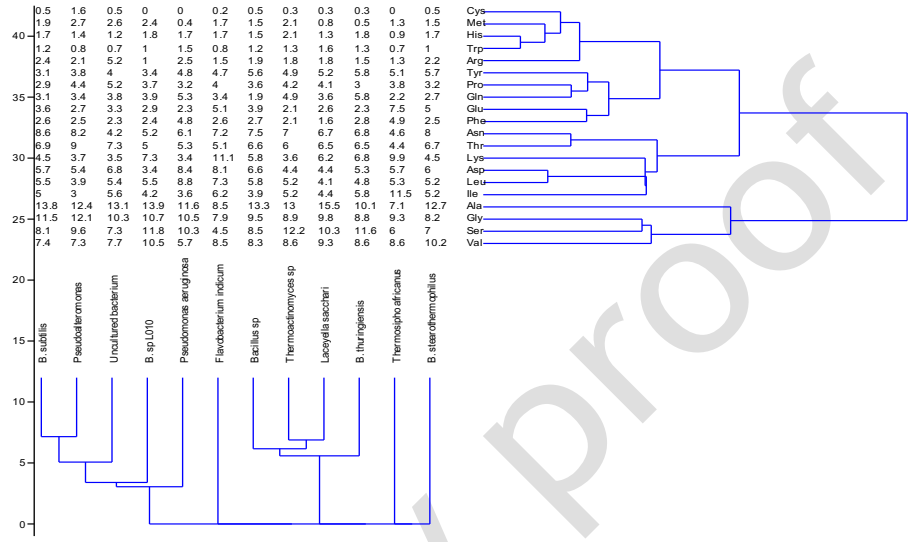

Supplementary figure: 3c.

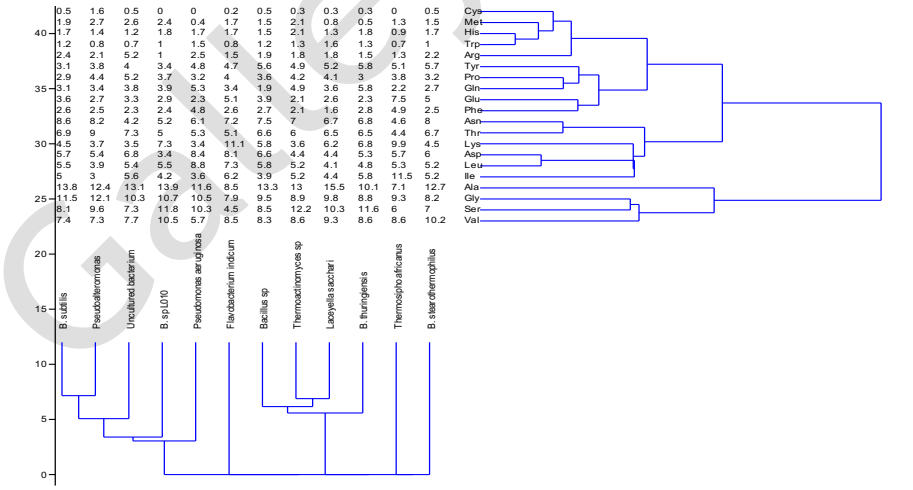

IIOAB JOURNAL
ISSN: 0976-3104

Supplementary figure: 3d.

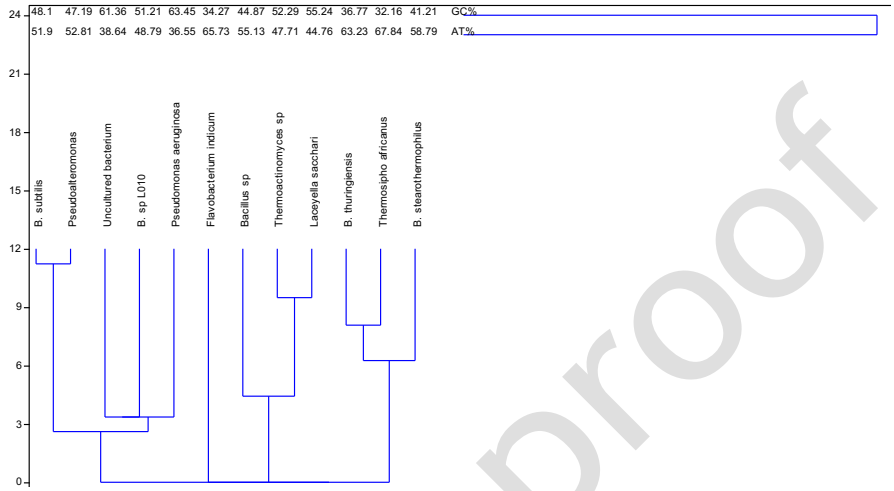

Supplementary figure: 3e

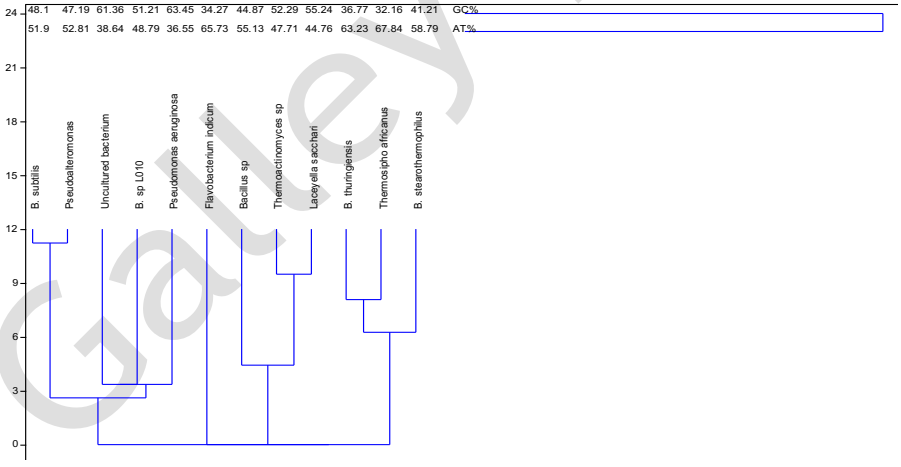

IIOAB JOURNAL
ISSN: 0976-3104

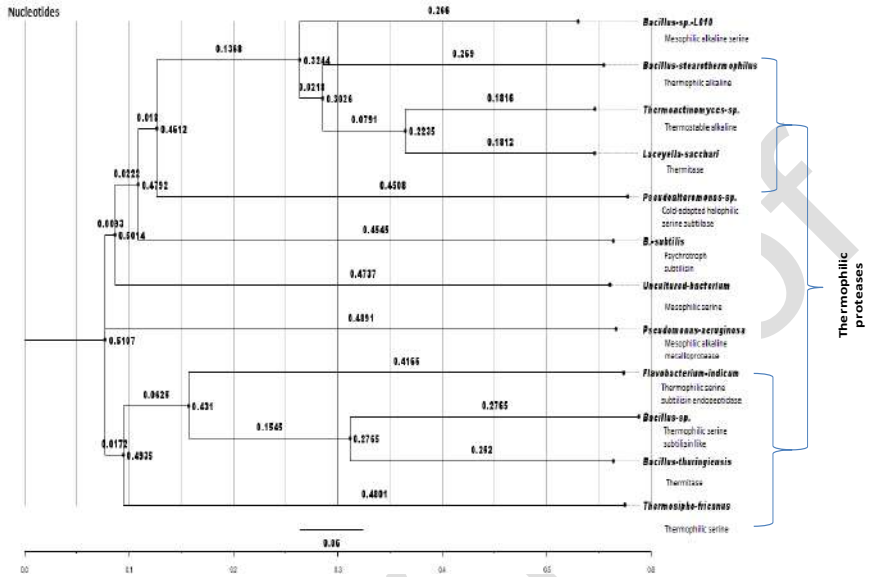

Nucleotides
0.266
Bacillus-sp.-LH9
Mesophilic alkaline serine
0.1368
0.3344
0.269
Bacillus-stearothermophilus
Thermophilic alkaline
0.3219
0.3026
0.1816
Thermoactinomyces-sp.
Thermostable alkaline
0.018
0.4612
0.0791
0.3235
0.1812
Laceyella-sacchari
Thermitase
0.0223
0.4752
0.4508
Pseudoalteromonas-sp.
Cold-adapted halophilic serine subtilase
0.0093
0.5014
0.4545
B.-subtilis
Psychrotroph subtilisin
0.4737
Uncultured-bacterium
Mesophilic serine
0.4851
Pseudomonas-aeruginosa
Mesophilic alkaline metalloprotease
0.5107
0.4166
Flavobacterium-indicum
Thermophilic serine subtilisin endopeptidase
0.0628
0.431
0.2765
Bacillus-sp.
Thermophilic serine subtilisin like
0.1548
0.0172
0.4935
0.2765
0.282
Bacillus-thuringiensis
Thermitase
0.4891
Thermosipho-fricanus
Thermophilic serine
Thermophilic proteases
0.06
0.0
0.1
0.2
0.3
0.4
0.5
0.6

IIOAB JOURNAL
ISSN: 0976-3104

Supplementary figure: 4. Multiple alignment of primary structure of twelve proteases' nucleotides. Shaded and less shaded represent conserved and highly conserved regions respectively

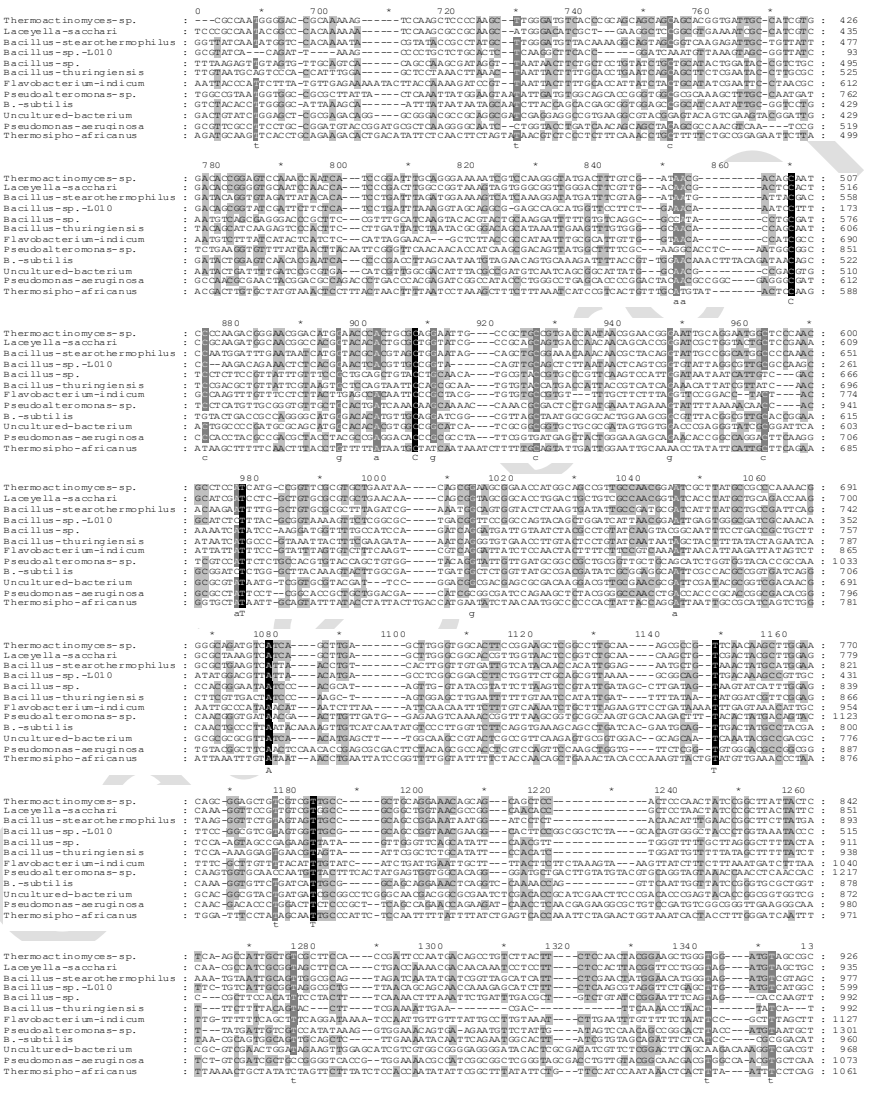

IIOAB JOURNAL
ISSN: 0976-3104

Supplementary figure: 5.Twelve protein models represent the twelve used proteases in this study. The source microbes are included in the Figure.

Bacillus stearothermophilus protease model

Thermosipho africanus protease model

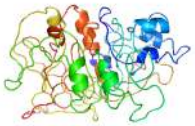

Bacillus sp. L010 protease model

Flavobacterium indicum protease model

Pseudoalteromonas sp. protease model

Pseudomonas aeruginosa protease model

B. subtilis protease model

Uncultured bacterium protease model

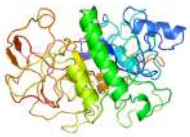

Laceyella sacchari protease model

Bacillus thuringiensis protease model

***Bacillus sp.* protease model**

***Thermoactinomyces sp.* protease model**

IIOAB JOURNAL
ISSN: 0976-3104

Supplementary figure: 6. Alignment of the twelve models in Fig: 5

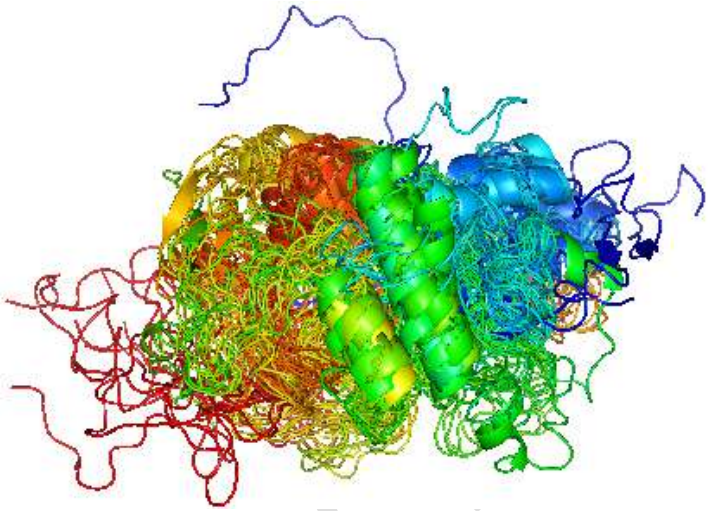

ISSN: 0976-3104
REGULAR ISSUE
Nair et al.

THE IIOAB JOURNAL

CASE REPORT OPEN ACCESS

DIAGNOSING THE ELUSIVE VRF USING CONE BEAM CT: CASE REPORTS

Manoj Nair, Jyoti Mandlik*, Pradeep Chaudhary

Department of Conservative Dentistry, Bharati Vidyapeeth Dental College, Pune, INDIA

ABSTRACT

Background: *Vertical root fracture (VRF) is one of the most difficult and perplexing conditions in clinical endodontics, to diagnose and treat. The fracture line is overlapped by different radio-opaque structures like the alveolar bone and root dentine in three dimensions that makes it very difficult to recognize on a traditional radiograph. The only other way to identify a vertical root fracture is to surgically expose the suspected site and visualize the defect.* ***Case description***: *The first case is of a 45year old male with periapical lesion in relation to 15 which was root canal treated 9 years ago. The swelling was asymptomatic and hence a fracture was suspected. The CBCT images confirmed the fracture on the axial sections. The second case is of a 52 year old male who reported with buccal swelling in relation to 36 which was endodontically treated 5years back. The location of the swelling was close to the marginal gingiva and in the furcation region. The intraoral radiograph showed halo type radiolucency, suggestive of VRF. The CBCT images confirmed the root fracture.* ***Discussion***: *The use of three-dimensional imaging has been prevalent in the medical field for a long time now and the dental fraternity is soon catching up. The introduction of CBCT in dentistry has opened up a wide range of applications for three-dimensional imaging at a fraction of the radiographic x-ray exposure. This newer method of acquiring hard tissue volume data has shown great promise. CBCT has been used for bone volume analysis for implants and surgical planning. Since the newer CBCT machines are capable of providing images with resolution as high as 90 microns, they could be used to detect vertical root fractures in the teeth without having to surgically expose the site. The application of CBCT in endodontics is increasing with the improved sensors and the sophisticated software to manipulate the volume data. A clear understanding of the data acquisition, the rendering process and the limitations of this diagnostic technique would help its applications in various other clinical aspects. Clinical significance: The use of CBCT to identify the presence of vertical root fracture would significantly reduce the prevailing ambiguity in the clinical diagnosis of VRF*

Received on: 24th-Sep-2014
Revised on: 29th-Oct-2014
Accepted on: 26th– Nov-2014
Published on: 4th –Dec-2014

KEY WORDS

CBCT; 3D Imaging; FOV; VRF; "Halo-appearance"

***Corresponding author:** Email: drjyoti8@gmail.com; Tel: + 91-9421385056

[I] INTRODUCTION

Vertical root fracture (VRF) is one of the most difficult and perplexing conditions in clinical endodontics, to diagnose and treat. Causes for VRF may include excessive mechanical root canal preparation, excessive forces during the compaction of root-filling materials, excessive canal widening for post placement, lack of periodontal support, internal resorptions or occlusion stress [1-4]. Identifying the presence of vertical root fractures (VRF) is often an endodontic challenge [5]. Clinical and radiographic evidence of the presence of root fractures does not always present itself until the fracture has been present for some time. However, even with long- standing VRF clinical signs of their existence maybe little more than a draining buccal sinus, which is certainly not pathognomonic of the problem. While a deep, isolated, thin periodontal pocket is suggestive of VRF, difficulty aligning the periodontal probe along the periodontal defect sometimes means this sign is missed [6]. Radiographic features suggestive of VRF such as J-shaped and halo-shaped radiolucencies do not appear until significant bone destruction has occurred and similarly shaped radiolucencies may manifest themselves in cases of apical periodontitis not associated with VRF. In this paper we present two cases of endodontically treated teeth with vertical root fracture diagnosed by CBCT imaging.

[II] CASE DESCRIPTION

2.1. Case 1

A 45 year old male patient reported to the clinic for evaluation of the upper right premolar with a buccal swelling. The tooth was endodontically treated 9 years ago. The patient did not complain of pain either on biting or spontaneously. He reported that he first noticed a small painless swelling about a month back which subsided on its own. It reoccurred few days back but was larger in size but still remained painless. Radiographic evaluation showed a fairly diffuse periodical radiolucency with apparent blunting of the root apex **[Figure– 1.1]**. The slight widening of the periodontal space all around the tooth suggested that the swelling was not purely periapical in nature. The patient was explained the possibility of a VRF and the possible diagnostic aids of surgical exploration and use of CBCT. The patient opted for the CBCT which was noninvasive in nature. The CBCT imaging was carried out using the Orthophos XG 3D by Sirona. The data acquired was then computed and rendered by the Galaxis software. The axial, coronal, and

THE IIOAB JOURNAL
ISSN: 0976-3104

sagittal sections were then studied to identify the fracture line. The Volume rendering image showed the fracture line **[Figure–1.2]**. The axial sections also showed the fracture line **[Figure–1.3]**. The images provided showed the presence of VRF on the buccal surface of the tooth. The results were then discussed with the patient and an informed decision to extract the tooth was taken. The tooth was extracted and the fracture was confirmed visually **[Figure–1.4]**.

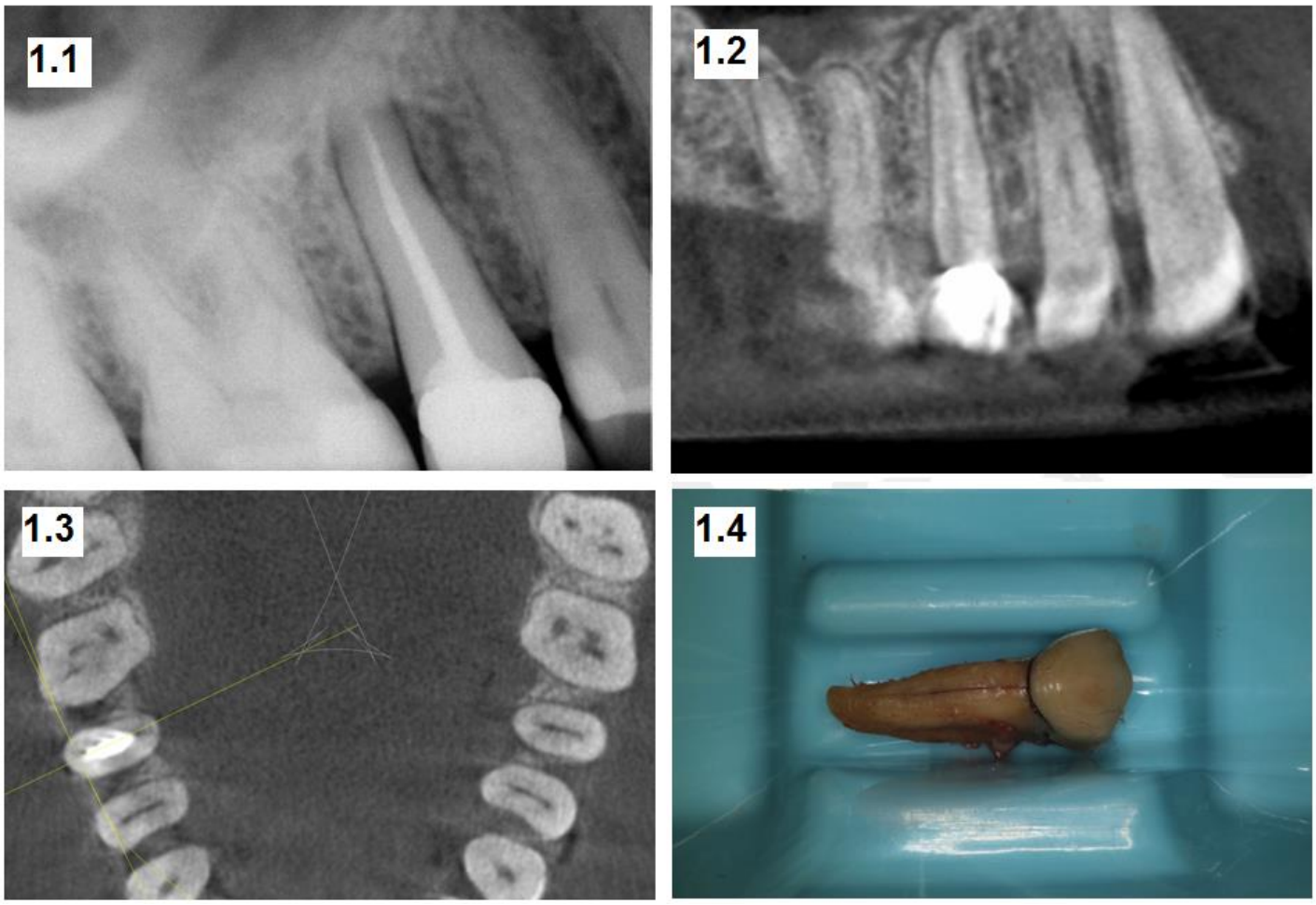

Fig: 1.1. Diagnostic radiograph; **Fig: 1.2.** CBCT Image longitudinal section showing fracture line; **Fig: 1.3.** Axial section of CBCT Image showing fracture; **Fig: 1.4.** Fracture evident after extraction

2.2. Case 2

A 52 year old male patient reported with a non painful buccal swelling in relation to 36 which recurred every few days since the last six months. The patient gave a history of root canal treatment about 5 years back. He did not complain of pain in the tooth but expressed some discomfort while biting on the side. Intraoral examination revealed the swelling to be closer to the furcation region. The intraoral radiograph showed radiolucency in the furcation and also along the length of the mesial root, the "halo" appearance **[Figure– 2.1]** suggestive of VRF. The patient was explained the possibility of a vertical root fracture and the treatment options. A CBCT Imaging was suggested to confirm the diagnosis of vertical root fracture as the patient wanted to avoid a surgery. The CBCT was carried out using the CS9300 by Carestream. The DICOM files were then computed using the Carestream software. The 3D volume rendering image and the various sections of the tooth was observed and the vertical root fracture was identified. The CBCT images showed the fracture on the mesial root **[Figure– 2.2, 2.3, 2.4, 2.5]**. The existing fracture line was then demonstrated to the patient and the need to extract the tooth to avoid further bone loss was also explained. The tooth was then extracted atraumatically and the fracture was visually identified **[Figure–2.6]**.

[III] DISCUSSION

Radiographic imaging is essential in diagnosis, treatment planning and follow-up in endodontics. The interpretation of an image can be confounded by a number of factors including the regional anatomy as well as superimposition of both the teeth and surrounding dento-alveolar structures. As a result of superimposition, periapical radiographs reveal only limited aspects, a two-dimensional view, of the true three-dimensional anatomy[7, 8].Additionally, there is often geometric distortion of the anatomical structures being imaged with conventional radiographic methods [9].These problems can be overcome by utilizing small- or limited-volume cone beam-computed

THE IIOAB JOURNAL
ISSN: 0976-3104

tomography imaging techniques, which produce accurate 3-D images of the teeth and surrounding dento-alveolar structures [7, 8, 10].CBCT provides precise, essentially immediate and accurate 3-D radiographic images. As CBCT exposure incorporates the entire FOV, only one rotational sequence of the gantry is necessary to acquire enough data for image reconstruction. At the present time, CBCT is considered a complementary modality for specific applications rather than a replacement for 2-D imaging modalities [10].

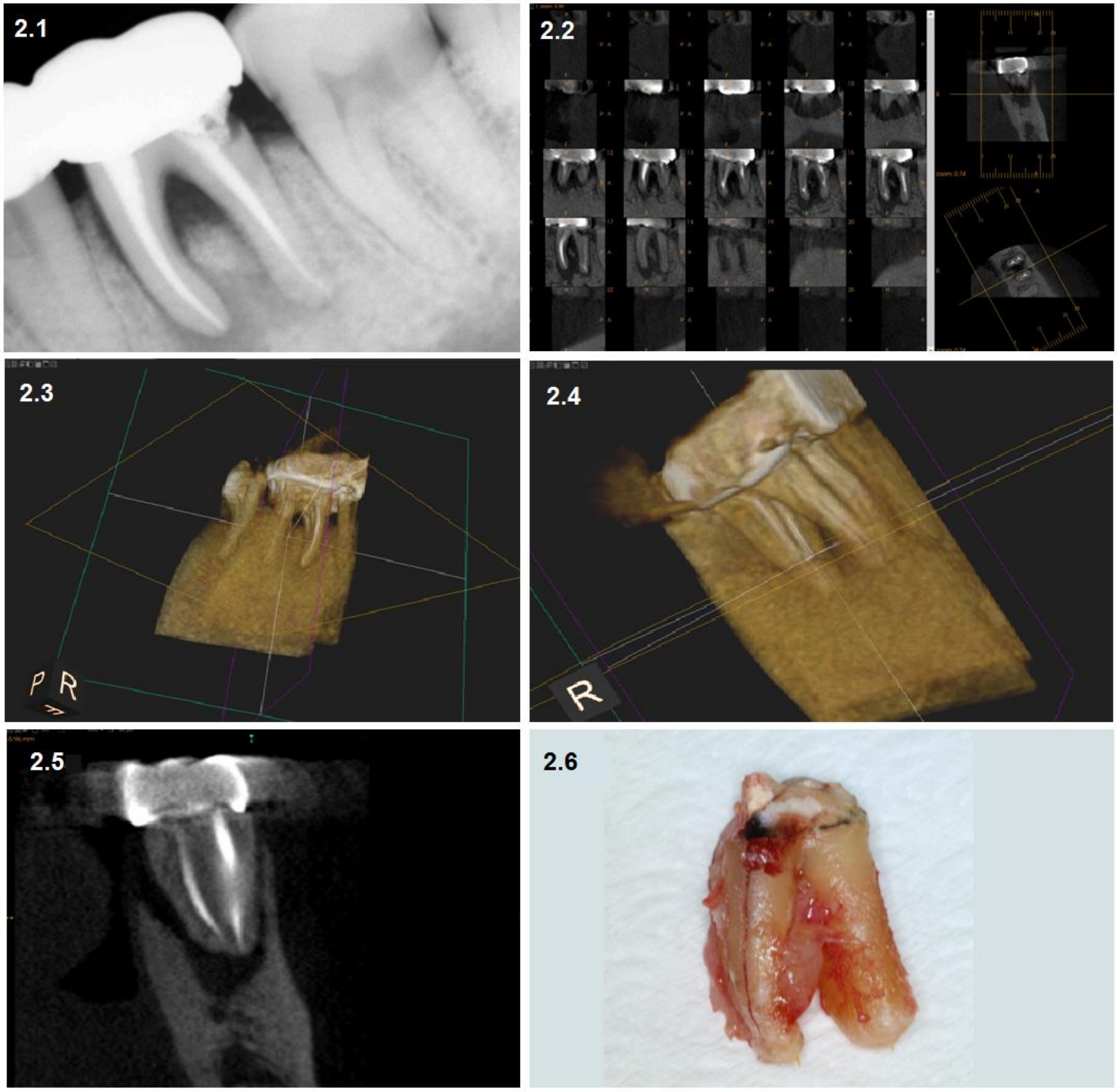

Fig: 2.1. Diagnostic radiograph; **Fig: 2.2.** CBCT Images showing sagittal / axial sections and fracture on mesial root; **Fig: 2.3. and 2.4.** CBCT Images showing oblique sections and fracture on mesial root; **Fig: 2.5.** CBCT Images showing oblique section and fracture on mesial root; **Fig: 2.6.** Fracture evident after extraction

THE IIOAB JOURNAL
ISSN: 0976-3104

Identifying the presence of vertical root fractures (VRF) is often an endodontic challenge [5]. Radiographic features suggestive of VRF such as J-shaped and halo-shaped radiolucencies do not appear until significant bone destruction has occurred and similarly shaped radiolucencies may manifest themselves in cases of apical periodontitis not associated with VRF. The most common radiographic feature of VRF is a halo radiolucency located on the lateral face of the root and extending to the periapical area, contrasting with the periapical radiolucency that remains surrounding only the periapex which is typical of the endodontic disease [9]. Radiographic angular bone loss and periodontal radiolucency may also be present in the VRF.

Lusting et al, from their extensive study on the cases of VRF, concluded that, the bone resorption, surrounding the fracture line on the bone plate, is consequential to VRF and it is due to the chronic inflammatory process where the granulation tissue replaces the bone following a bacterial infection that was able to gain an easy passage through the fracture line bypassing the defense line of the epithelial attachment. The same authors propose, after a correct VRF diagnosis, the extraction of the tooth without delay to prevent a more severe resorption of the bone plate [11]. Four standard procedures have been described to allow a correct and definitive diagnosis of VRF: a visualization during an exploratory surgery, a visualization after tooth extraction, a radiographic visualization as long as there is a separation of fragments, [12] and a Cone Beam Computer Tomography visualization of the fracture.[13,14] Ex vivo studies have demonstrated that CBCT is more sensitive than conventional radiography in the detection of vertical fractures in roots .However, care should be taken when assessing root filled teeth for VRF using CBCT as scatter produced by the root filling or other high-density intraradicular material may incorrectly suggest the presence of a fracture [14].

The use of CBCT technology in clinical practice provides a number of potential advantages for maxillofacial imaging [15]:

- **X-ray beam limitation:** Reducing the size of the irradiated area by collimation of the primary x-ray beam to the area of interest minimizes the radiation dose. Most CBCT units can be adjusted to scan small regions for specific diagnostic tasks.
- **Image accuracy:** The volumetric data set comprises a 3D block of smaller cuboid structures, known as voxels, each representing a specific degree of x-ray absorption. The size of these voxels determines the resolution of the image. All CBCT units provide voxel resolutions that are isotropic — equal in all 3 dimensions. This produces sub-millimetre resolution (often exceeding the highest grade multi-slice CT) ranging from 0.4 mm to as low as 0.125 mm (Accuitomo).
- **Rapid scan time:** Because CBCT acquires all basis images in a single rotation, scan time is rapid (10–70 seconds) and comparable with that of medical spiral MDCT systems. Although faster scanning time usually means fewer basis images from which to reconstruct the volumetric data set, motion artifacts due to subject movement are reduced.
- **Dose reduction:** Published reports indicate that the effective dose of radiation (average range 36.9–50.3 microsievert [μSv]) is significantly reduced by up to 98% compared with "conventional" fan-beam CT systems (average range for mandible 1,320–3,324 μSv; average range for maxilla 1,031–1,420 μSv). This reduces the effective patient dose to approximately that of a film-based periapical survey of the dentition (13–100 μSv) or 4–15 times that of a single panoramic radiograph (2.9–11 μSv).

[IV] CONCLUTION

This paper highlights the potential uses of CBCT in the assessment and management of common endodontic problems like VRF. This three-dimensional imaging technique overcomes the limitations of conventional radiography and is a beneficial adjunct to the endodontist's armamentarium. Nevertheless, the effective radiation dose to patients when using CBCT is higher than in conventional intraoral radiography and any benefit to the patient of CBCT scans should outweigh any potential risks of the procedure, in order to be justified. The radiation should be as low as reasonably achievable (ALARA). The decision to prescribe CBCT scans in the management of endodontic problems must be made on a case-by-case basis and only when sufficient diagnostic information is not attainable from other diagnostic tests, be they clinical or radiographic.

CONFLICT OF INTEREST

The authors declare that they have no conflicts of interest.

ACKNOWLEDGEMENT

We acknowledge patient's cooperation and appreciate their involvement in decision making about the CBCT imaging technique used as a diagnostic tool.

FINANCIAL DISCLOSURE

The cases presented in this article were conducted at the private practice of the authors and were not supported by any financial assistance.

.

REFERENCES

[1] Tamse A. [2006] Vertical root fractures in endodontically treated teeth: diagnostic signs and clinical management. *Endod Top* 13:84–94.

[2] Llena-Puy M, Navarro L, Navarro I. [2001] Vertical root fracture in endodontically treated teeth: a review of 25 cases. *Oral Surg Oral Med Oral Pathol Oral RadiolEndod* 92:553–555.

[3] Barreto M, Moraes R, Rosa R, Moreira C, Vinicius M, Bier C. [2012]Vertical root fractures and dentin defects: effects of root canal preparation, filling and mechanical cycling. *J Endod* 38:1135–1139.

[4] Lertchirakarn V, Palamara J, Messer H. [1999] Load and strain during lateral condensation and vertical root fracture. *J Endod* 25:99–104.

[5] Tamse A, Fuss Z, Lustig J, Kaplavi J. [1999] An evaluation of endodontically treated vertically fractured teeth. *J Endod* 25:506–508.
[6] Tamse A, Kaffe I, Lustig J, Ganor J, Fuss Z. [2006] Radiographic features of vertically fractured endodontically treated mesial roots of mandibular molars. *Oral Surg Oral Med Oral Pathol Oral RadiolEndod* 101:797–802.
[7] Patel S, Dawood A, Pitt Ford T, Whaites E. [2007] The potential applications of cone beam computed tomography in the management of endodontic problems. *IntEndod j* 40:818–830.
[8] Cotton TP, Geisler TM, Holden DT, Schwartz SA, Schindler WG.[2007] Endodontic applications of cone beam volumetric tomography. *J Endod*; 33:1121–1132.
[9] Grondahl HG, Huumonen S.[2004] Radiographic manifestations of periapical inflammatory lesions. *Endod Topics* 8:55–67.
[10] Scarfe WC, Levin MD, Gane D, Farman AG. [2009] Use of cone beam computed tomography in endodontics. *Int J Dent*: 2009; 634567.
[11] Lustig J, Tamse A, Fuss Z. [2000] Pattern of bone resorption in vertically fractured, endodontically treated teeth. *Oral Surg Oral Med Oral Pathol Oral RadiolEndod* 90:224–227.
[12] Tsesis I, Rosen E, Tamse A, Taschieri S, Kfir A. [2010] Diagnosis of vertical root fractures in endodontically treated teeth based on clinical and radiographic indices: a systematic review. *J Endod* 36:1455–1458.
[13] Edlund M, Nair M, Nair U. [2011] Detection of vertical root fractures by using cone-beam computer tomography: a clinical study. *J Endod* 37:768–772.
[14] Hassan B, Metska M, Ozok A, Selt P, Wesselink P. [2009] Detection of vertical root fractures in endodontically treated teeth by cone beam computer tomography scan. *J Endod* 35:719–722.
[15] Scarfe WC, Farman AG. [2006]Clinical Applications of Cone-Beam Computed Tomography in Dental Practice. *J Can Dent Assoc* 72(1):75–80.

ABOUT AUTHORS

Prof. Dr. Manoj Nair *is post graduate teacher and guide in the department of Conservative Dentistry and Endodontics at Bharati Vidyapeeth Deemed University's Dental College and Hospital Pune, India*

Dr. Jyoti Mandlik *is Associate Professor in the department of Conservative Dentistry and Endodontics at Bharati Vidyapeeth Deemed University's Dental College and Hospital Pune, India*

Prof. Dr. Pradeep Chaudhari *is post graduate teacher and guide in the department of Conservative Dentistry and Endodontics at Bharati Vidyapeeth Deemed University's Dental College and Hospital Pune, India*